

LncRNA LITATS1 suppresses TGF- β -induced EMT and cancer cell plasticity by potentiating T β RI degradation

Chuannan Fan^{1,2} , Qian Wang^{1,2} , Thomas B Kuipers³ , Davy Cats³ ,
Prasanna Vasudevan Iyengar^{1,2} , Sophie C Hagenaars⁴ , Wilma E Mesker⁴ , Peter Devilee^{5,6} ,
Rob A E M Tollenaar⁴ , Hailiang Mei³  & Peter ten Dijke^{1,2,*} 

Abstract

Epithelial cells acquire mesenchymal phenotypes through epithelial-mesenchymal transition (EMT) during cancer progression. However, how epithelial cells retain their epithelial traits and prevent malignant transformation is not well understood. Here, we report that the long noncoding RNA *LITATS1* (*LINC01137*, *ZC3H12A-DT*) is an epithelial gatekeeper in normal epithelial cells and inhibits EMT in breast and non-small cell lung cancer cells. Transcriptome analysis identified *LITATS1* as a TGF- β target gene. *LITATS1* expression is reduced in lung adenocarcinoma tissues compared with adjacent normal tissues and correlates with a favorable prognosis in breast and non-small cell lung cancer patients. *LITATS1* depletion promotes TGF- β -induced EMT, migration, and extravasation in cancer cells. Unbiased pathway analysis demonstrated that *LITATS1* knockdown potently and selectively potentiates TGF- β /SMAD signaling. Mechanistically, *LITATS1* enhances the polyubiquitination and proteasomal degradation of TGF- β type I receptor (T β RI). *LITATS1* interacts with T β RI and the E3 ligase SMURF2, promoting the cytoplasmic retention of SMURF2. Our findings highlight a protective function of *LITATS1* in epithelial integrity maintenance through the attenuation of TGF- β /SMAD signaling and EMT.

Keywords epithelial-mesenchymal transition; *LINC01137*; TGF- β type I receptor; transforming growth factor- β ; *ZC3H12A-DT*

Subject Categories Cancer; RNA Biology

DOI 10.15252/embj.2022112806 | Received 13 October 2022 | Revised 28 February 2023 | Accepted 2 March 2023 | Published online 30 March 2023

The EMBO Journal (2023) 42: e112806

Introduction

At the early stage of epithelium-derived cancers, highly polarized epithelial cells gradually lose cell-cell adhesion and acquire mesenchymal-like features through a process called epithelial-mesenchymal transition (EMT; Pastushenko & Blanpain, 2019; Gui & Bivona, 2022; Hanahan, 2022). This process is characterized by the loss of epithelial markers (E-cadherin, ZO-1, etc.) and the gain of mesenchymal markers (Fibronectin, N-cadherin, Vimentin, etc.) in epithelial cells. Mesenchymal cancer cells can invade through the basement membrane and intravasate into the vascular circulation, resulting in the dissemination of cancer cells and the formation of metastases in distant organs (Hanahan, 2022). However, the reversible EMT process includes multiple intermediate states, referred to as partial or hybrid EMT (Sha *et al.*, 2019; Yang *et al.*, 2020). In particular, cancer cells with a dynamic epithelial-mesenchymal plasticity (EMP) phenotype demonstrate greater malignancy, more prominent stem cell characteristics, and greater resistance to chemotherapy (Shibue & Weinberg, 2017; van Staalduinen *et al.*, 2018; Dongre & Weinberg, 2019; Yang *et al.*, 2020).

Signaling by the secreted cytokine transforming growth factor β (TGF- β) is a main EMT driver, and targeting proactive TGF- β signaling for cancer treatment has been evaluated clinically (Colak & ten Dijke, 2017; Fan *et al.*, 2018; Hao *et al.*, 2019). TGF- β initiates signaling upon binding to complexes of TGF- β type I and type II serine/threonine receptors (T β RI and T β RII, respectively). Activated T β RI induces regulated (R)-SMAD2/3 phosphorylation, after which phosphorylated SMAD2/3 translocates into the nucleus by forming complexes with SMAD4. These SMAD complexes regulate gene transcription by cooperating with other transcription factors (Hata & Chen, 2016; Tzavlaki & Moustakas, 2020). The intensity and duration of TGF- β signaling are finely tuned at multiple levels (Yan *et al.*, 2018). At the receptor level, SMAD-Specific E3 Ubiquitin

1 Department of Cell and Chemical Biology, Leiden University Medical Center, Leiden, The Netherlands

2 Oncode Institute, Leiden University Medical Center, Leiden, The Netherlands

3 Department of Biomedical Data Sciences, Sequencing Analysis Support Core, Leiden University Medical Center, Leiden, The Netherlands

4 Department of Surgery, Leiden University Medical Centre, Leiden, The Netherlands

5 Department of Pathology, Leiden University Medical Center, Leiden, The Netherlands

6 Department of Human Genetics, Leiden University Medical Center, Leiden, The Netherlands

*Corresponding author. Tel: +31 71 526 9271; Fax: +31 71 526 8270; E-mail: p.ten_dijke@lumc.nl

Protein Ligase 1/2 (SMURF1/2) are recruited to activated T β RI by interacting with the inhibitory protein SMAD7 and thereby polyubiquitinate and degrade T β RI (Kavsak *et al.*, 2000; Budi *et al.*, 2017).

Long noncoding RNAs (lncRNAs) are defined as transcripts that are longer than 200 nucleotides, transcribed by RNA polymerase II, and lack the protein-coding ability (Mattick & Rinn, 2015; Palazzo & Koonin, 2020). The regulatory functions of lncRNAs in various biological processes and pathological events, including cancer progression, have been shown (Nandwani *et al.*, 2021; Statello *et al.*, 2021). lncRNAs can serve as guides, scaffolds or decoys to modulate the interactions between biological macromolecules, such as protein–protein interactions and protein–DNA interactions, and thereby regulate gene expression at multiple levels (Lin & Yang, 2018; Palazzo & Koonin, 2020). In addition, lncRNAs can sponge microRNAs (miRNAs) by acting as competitive endogenous RNAs (ceRNAs; Tay *et al.*, 2014; Thomson & Dinger, 2016).

Epithelial cells protect their integrity by sustaining the expression of epithelial gatekeeper proteins such as OVOL1/2 (Watanabe *et al.*, 2014), GRHL2 (Chung *et al.*, 2019), and C/EBP α (Lourenco *et al.*, 2020). Loss of these proteins induces epigenetic reprogramming and/or hyperactivation of EMT-promoting transcription factors or signaling pathways, resulting in the disruption of epithelial integrity and the acquisition of mesenchymal features (Watanabe *et al.*, 2014; Chung *et al.*, 2019; Fan *et al.*, 2022). lncRNAs are emerging as a new class of EMT regulators. By functioning as an epigenetic silencer, human HOX antisense intergenic RNA (*HOTAIR*) suppresses EMT and breast cancer metastasis (Jarroux *et al.*, 2021; Ma *et al.*, 2022). However, whether lncRNAs participate in maintaining epithelial architecture is poorly understood. Here, we identify lncRNA Induced by TGF- β and Antagonizes TGF- β Signaling 1 (*LITATS1*) as a protector of epithelial cells to inhibit TGF- β -induced EMT and invasive abilities. Our findings reveal a novel lncRNA-directed mechanism by which epithelial cells maintain their integrity and thereby prevent TGF- β -induced EMT and cancer cell invasion.

Results

LITATS1 is a cytoplasmic lncRNA whose expression is induced by TGF- β /SMAD signaling

TGF- β is a pivotal driver of EMT that disrupts epithelial integrity (Fan *et al.*, 2018; Hao *et al.*, 2019). To investigate the role of lncRNAs in TGF- β -induced EMT and cell migration, we performed transcriptional profiling to screen for TGF- β -induced lncRNAs in breast cell lines that respond to TGF- β -induced EMT (i.e., MCF10A-M1 normal breast epithelial cells and MCF10A-M2 premalignant breast cells; Appendix Fig S1A–C) or in which TGF- β stimulates cell migration and invasion (i.e., MDA-MB-231 mesenchymal triple-negative breast cancer cells; Appendix Fig S1A, B and D). RNA sequencing (RNA-seq) analysis was performed on these three cell lines stimulated with TGF- β for short (2 h), moderate (8 h), and prolonged (24 h) durations (Fig 1A). Using samples without TGF- β treatment (0 h) as the reference, we selected 15 lncRNAs whose expression is decent among the 25 lncRNAs that were induced by TGF- β in at least two of the three cell lines after all TGF- β stimulation durations ($P < 0.05$, fold change >2 ; Fig 1B, Appendix Fig S1E, Table S1). Analysis of a separate batch of RNA samples from MCF10A-M2 cells

validated the induction of these 15 lncRNA hits by TGF- β (Appendix Fig S1F). Moreover, 9 of the 15 lncRNAs were also potentially upregulated by TGF- β in A549 lung adenocarcinoma cells, a cell line that is commonly used to investigate TGF- β -induced EMT (Appendix Fig S2A). A further screen directed by individually depleting the 9 lncRNAs with two independent GapmeRs identified two lncRNAs (No. 4 and No. 11; Appendix Table S1) whose knockdown augmented TGF- β -mediated effects on the rearrangement of the actin cytoskeleton into filamentous (F)-actin stress fibers and EMT marker expression (Appendix Fig S2B–D). We observed that one unannotated lncRNA (No. 12; Appendix Table S1) exerted the opposite effects (Appendix Fig S2B–D). As a well-characterized lncRNA, lncRNA No. 4 (*NKILA*) was reported to be induced by TGF- β and alleviate EMT and cancer metastasis (Liu *et al.*, 2015; Lu *et al.*, 2017; Wu *et al.*, 2018). We prioritized lncRNA No. 11 (which we termed *LITATS1*) for further investigation due to its abundant basal and prominent TGF- β -induced expression (Appendix Figs S1F and S2A) and its potent inhibitory effects on TGF- β -induced EMT (Appendix Fig S2C and D).

To evaluate *LITATS1* kinetic expression pattern upon TGF- β treatment, we prolonged the duration of TGF- β stimulation and observed a sustained *LITATS1* expression until 72 h in MDA-MB-231 and A549 cells (Fig EV1A). To verify and extend our identification of *LITATS1* as a TGF- β -induced target gene, we depleted SMAD4 in MDA-MB-231 cells and found that both basal and TGF- β -induced *LITATS1* expression levels were mitigated (Figs 1C and EV1B). Moreover, *LITATS1* expression was enhanced upon ectopic expression of constitutively active TGF- β type I receptor (caT β RI) in HEK293T cells (Fig 1D). To further investigate the mechanism by which TGF- β /SMAD signaling potentiates *LITATS1* expression, the *LITATS1* promoter was characterized. TGF- β but not the closely related family member bone morphogenetic protein (BMP)6, stimulated the transcriptional activity of the *LITATS1* promoter fragment (–3,387 to –1,585 bp upstream of the transcription start site; chromosome 1: 37,476,029 to 37,477,830 (GRCh38.p14)) when placed upstream of a luciferase reporter gene (Figs 1E and EV1C). In addition, ectopic expression of caT β RI or its downstream transcriptional effector SMAD3 (in either the absence or presence of exogenous TGF- β) enhanced *LITATS1* promoter activity (Fig EV1D). Next, transcriptional activity analysis of *LITATS1* promoter truncation mutants demonstrated that the promoter region containing bp –3,212 to –2,649 (chromosome 1: 37,477,093 to 37,477,655 (GRCh38.p14)) was responsible for the TGF- β -mediated transcriptional activity (Fig EV1E). Notably, mutation of a putative SMAD binding site completely abrogated basal and TGF- β -driven *LITATS1* transcription (Figs 1F and EV1F). Collectively, our results reveal that *LITATS1* is a direct target gene of TGF- β /SMAD signaling.

Next, we mapped the *LITATS1* locus on chromosome 1, which is located at head-to-head orientation to a protein-coding gene *ZC3H12A* (Fig 1G). The 5' and 3' rapid amplification of cDNA ends (RACE) assays demonstrated that *LITATS1* is a 1,443 nt three-exon transcript that is identical to an annotated lncRNA *LINC01137* in the NCBI database or *ZC3H12A-DT* in the Ensembl database (Figs 1G and EV1G). Although *LITATS1* is shown as the only splice variant in the NCBI database, *ZC3H12A-DT* was found to be spliced into seven splice variants as shown in the Ensembl database (Appendix Fig S3A). To check whether *LITATS1* (splice variant 1) is the only TGF- β -induced *ZC3H12A-DT* splice variant, we analyzed the RNA-seq data and estimated the raw sequencing reads using StringTie

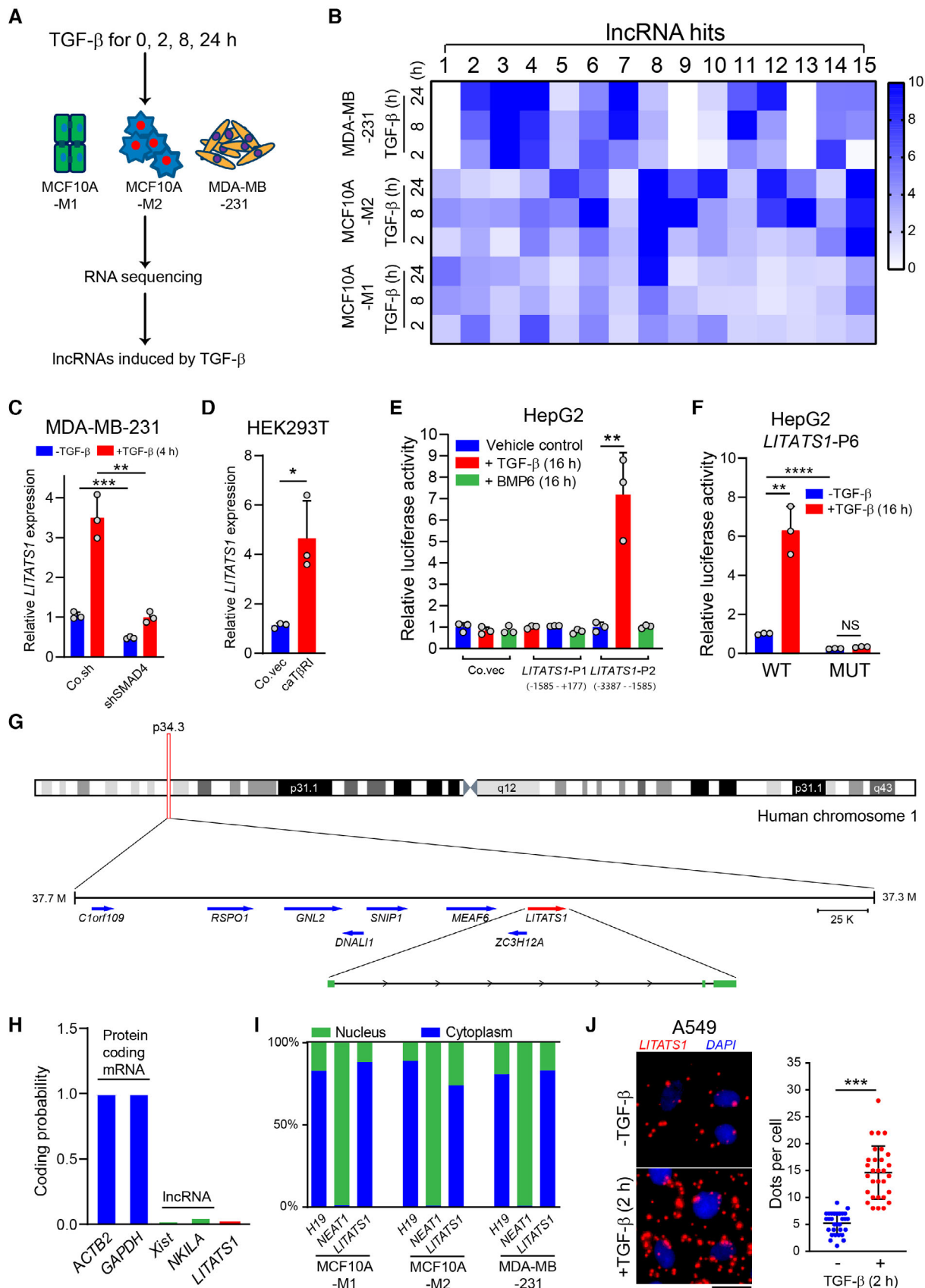


Figure 1.

Figure 1. *LITATS1* is a TGF- β -induced lncRNA.

- A Scheme for screening lncRNAs induced by TGF- β . MCF10A-M1, MCF10A-M2, and MDA-MB-231 cells were treated without (0 h) or with TGF- β for 2 h, 8 h, or 24 h. RNA samples (biological triplicates) were collected for RNA-seq, and lncRNAs induced by TGF- β were selected for further analysis.
- B Heatmap showing the log₂ fold changes in the 15 lncRNA hits induced by TGF- β at all three time points (2 h, 8 h, and 24 h vs. 0 h) in at least two cell lines.
- C *LITATS1* expression upon *SMAD4* knockdown (as detected by RT-qPCR) in MDA-MB-231 cells. Cells were serum starved for 16 h and TGF- β was added for 4 h. Representative results from a minimum of three independent experiments are shown.
- D *LITATS1* expression (as detected by RT-qPCR) in HEK293T cells. Cells were transfected without (Co.vec) or with the constitutively active TGF- β type I receptor (caT β RI) ectopic expression construct. Representative results from a minimum of three independent experiments are shown.
- E Effect of TGF- β on *LITATS1* promoter activity as determined by luciferase reporter assays. HepG2 cells were transfected with empty pGL4 vector (Co.vec) or with two indicated *LITATS1* promoter luciferase reporters (*LITATS1*-P1 and *LITATS1*-P2). Cells were stimulated with ligand buffer as the vehicle control (–), BMP6 (50 ng/ml), or TGF- β (5 ng/ml) for 16 h. Representative results from a minimum of three independent experiments are shown.
- F Effect of caT β RI and *SMAD3* on *LITATS1* promoter activity as determined by luciferase reporter assays. HepG2 cells were transfected with ectopic expression constructs for the *LITATS1* promoter 2 luciferase reporter (*LITATS1*-P2) and caT β RI or *SMAD3* and were then stimulated with or without TGF- β for 16 h. Representative results from a minimum of three independent experiments are shown.
- G Schematic representation of the genomic location of *LITATS1* and its neighboring genes. The arrows indicate the direction of transcription.
- H CPAT software was used to predict the coding potential of protein-coding mRNAs (*ACTB2* and *GAPDH*), well-annotated lncRNAs (*Xist* and *NKILA*), and *LITATS1*.
- I Expression analysis of lncRNA *H19*, *NEAT1*, and *LITATS1* expression levels in the cytoplasmic and nuclear fractions of MCF10A-M1, MCF10A-M2, and MDA-MB-231 cells. Representative results from a minimum of three independent experiments are shown.
- J RNA fluorescence *in situ* hybridization was performed to evaluate *LITATS1* expression and subcellular localization in A549 cells. Cells were treated with or without TGF- β for 2 h. Representative images are shown in the left panel, and signal quantification data are shown in the right panel. Scale bar = 10 μ m. Representative results from two independent experiments are shown.

Data information: TGF- β was applied at a final concentration of 5 ng/ml. (C, D, E, F) are expressed as the mean \pm SD values from three biological replicates ($n = 3$). (J) is expressed as the mean \pm SD values from 30 biological replicates ($n = 30$). * $0.01 < P < 0.05$; ** $0.001 < P < 0.01$; *** $0.0001 < P < 0.001$; **** $P < 0.0001$; NS, not significant. Statistical analysis was based on the unpaired Student's *t*-test.

Source data are available online for this figure.

that can discriminate the seven splice variants. We found that *LITATS1* (splice variant 1) basal expression was the highest among the seven splice variants (Appendix Fig S3B). Moreover, *LITATS1* (splice variant 1) was the only variant that can be induced by TGF- β in all three breast cell lines (Appendix Fig S3B). Additionally, reverse transcription-quantitative PCR (RT-qPCR) analysis of MDA-MB-231 and A549 cells consolidated this result (Appendix Fig S3C and D).

Bioinformatic analysis with Coding Potential Assessment Tool (CPAT; Wang *et al.*, 2013) predicted that *LITATS1* lacked coding potential (Fig 1H). As the subcellular localization of lncRNAs aids in deciphering their functions and mechanisms, subcellular fractionation followed by RT-qPCR was carried out. As shown in Fig 1I, *LITATS1* was localized mainly in the cytoplasm (73.9–88.1%) of three breast cell lines, which was confirmed by fluorescence *in situ* hybridization in A549 cells (Figs 1J and EV1H). Moreover, TGF- β

stimulation did not alter the cytoplasmic and nuclear distribution of *LITATS1* (Fig EV1I). Collectively, these results reveal that *LITATS1* is a cytoplasmic lncRNA whose expression is induced by TGF- β /SMAD signaling.

***LITATS1* expression correlates with a better outcome in cancer patients**

To explore the relationship between *LITATS1* and EMT, *LITATS1* expression was initially analyzed in a panel of breast cell lines with epithelial and/or mesenchymal features. Two mesenchymal-like breast cancer cell lines, MDA-MB-231 and MDA-MB-436, displayed less *LITATS1* expression than three epithelial-like cell lines (MCF10A-M1, MCF10A-M2, and MCF7; Fig 2A). In addition, analysis of RNA-seq data from the TCGA (Koboldt *et al.*, 2012) and GTEx (Lonsdale *et al.*, 2013) breast cancer datasets revealed that *LITATS1*

Figure 2. *LITATS1* expression correlates with better prognosis in breast cancer and lung cancer patients.

- A *LITATS1* expression in different breast cells as measured by RT-qPCR. Results from epithelial-like and mesenchymal-like cells are labeled in blue and green, respectively. Representative results from two independent experiments are shown.
- B Comparison of *LITATS1* expression in breast cancer classified by PAM50 subtypes.
- C Quantification of *LITATS1* expression levels by *in situ* hybridization in lung adenocarcinoma tissue microarrays. Representative images (bar = 100 μ m) and zoomed images (bar = 20 μ m) of *in situ* hybridization results in lung adenocarcinoma and matched adjacent normal tissues are shown in the left panel. The comparison of the *LITATS1* staining index between the paired tissues is shown in the right panel. Tissue pairs with higher *LITATS1* expression in the normal tissue (normal) than in the lung adenocarcinoma tissue (tumor) are highlighted in red, whereas tissue pairs with lower *LITATS1* expression in the normal tissue than in the tumor tissue are highlighted in green.
- D Kaplan–Meier survival curves of relapse-free survival in 175 breast cancer patients stratified by *LITATS1* expression. *LITATS1* expression was measured by *in situ* hybridization in breast cancer tissue microarrays.
- E–H Kaplan–Meier survival curves of overall survival (E), distant metastasis-free survival (F), and relapse-free survival (G) in breast cancer patients and overall survival (H) in non-small cell lung cancer patients stratified by *LITATS1* expression. The data were generated via Kaplan–Meier Plotter (<https://kmplot.com/analysis/>).

Data information: (A) is expressed as the mean \pm SD values from three biological replicates ($n = 3$). (B) is represented as box-and-whisker plots with 5–95 percentile line representing the median of each group. Numbers below the plot represent patient numbers (biological replicates). (C) is expressed as the mean \pm SD values from 49 biological replicates ($n = 49$). * $0.01 < P < 0.05$; ** $0.001 < P < 0.01$; **** $P < 0.0001$. In (A, B), statistical analysis was based on the unpaired Student's *t*-test. In (C), statistical analysis was based on the paired Student's *t*-test. In (D–H), the log-rank (Mantel-Cox) test was applied to calculate the statistical significance.

Source data are available online for this figure.

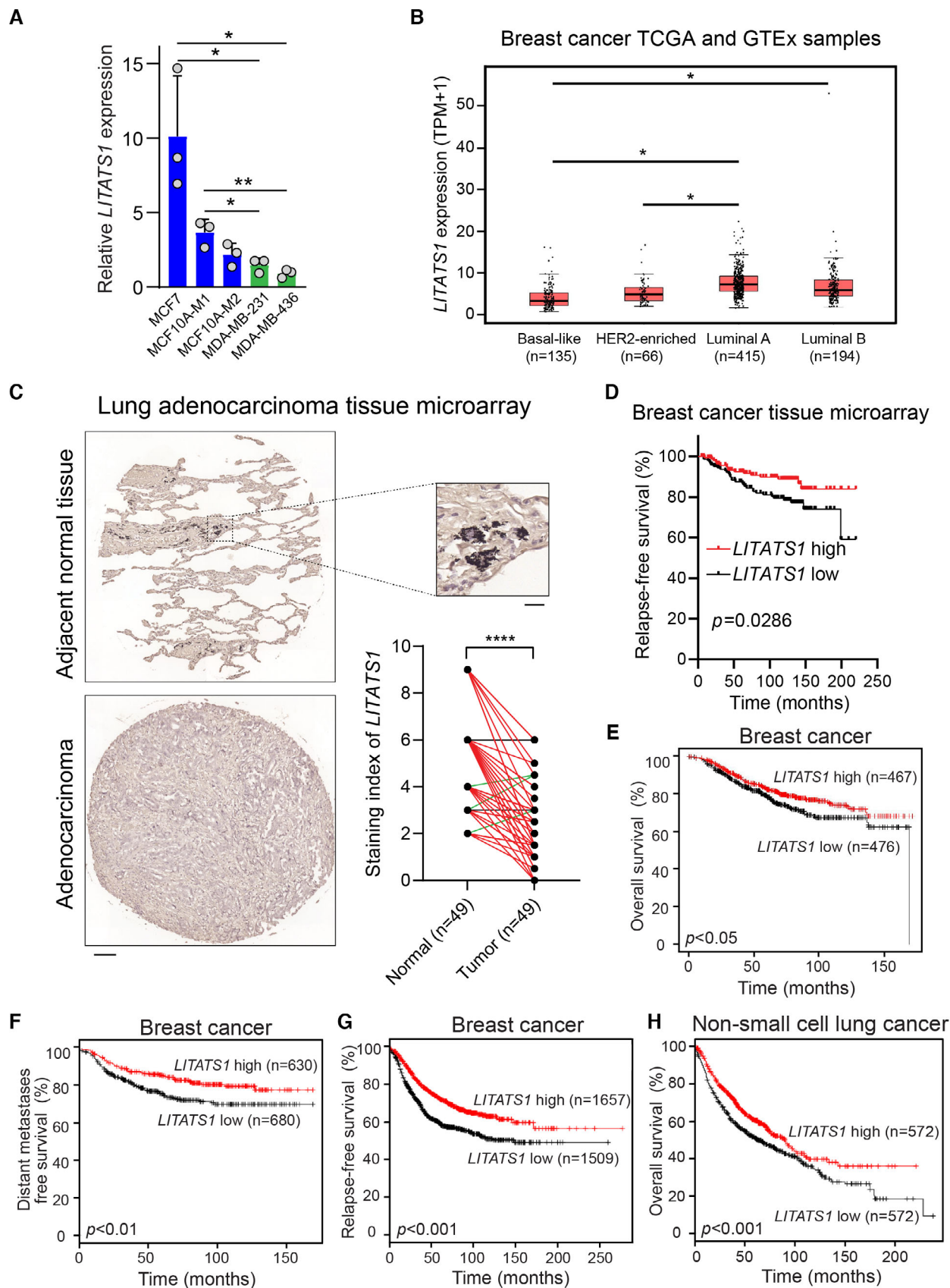


Figure 2.

expression was significantly decreased in patient samples classified into the basal-like and HER2-enriched subtypes with poor prognosis compared with the luminal A and luminal B subtypes with better prognosis (Parker *et al*, 2009; Fig 2B). Moreover, *in situ* hybridization with a *LITATS1* probe in a commercial tissue microarray showed that *LITATS1* expression was reduced in lung adenocarcinoma samples compared with matched adjacent normal samples, with a lower level in 89.8% (44 of 49) of the tested samples (Fig 2C). To investigate the correlation between *LITATS1* expression and survival in patients with breast cancer, a Kaplan–Meier plot was generated based on the *in situ* hybridization results in the ORIGO breast cancer tissue microarray (Out *et al*, 2012). Higher *LITATS1* expression was associated with a higher relapse-free survival rate ($P = 0.0286$) in the cohort of 175 breast cancer patients (Fig 2D). Furthermore, bioinformatic Kaplan–Meier analysis using other patient cohorts (Gyorffy *et al*, 2014; Gyorffy, 2021) also revealed that high *LITATS1* expression correlated with a favorable outcome in breast and non-small cell lung cancer patients (Fig 2E–H). Together, our results demonstrate that *LITATS1* is expressed at lower levels in mesenchymal breast cancer cells and that *LITATS1* expression correlates with a favorable clinical outcome in breast and non-small cell lung cancer patients.

Loss of *LITATS1* potentiates TGF- β -induced EMT and cell migration

To further investigate the impact of *LITATS1* on TGF- β -induced EMT, *LITATS1* was overexpressed by CRISPR activation (CRISPRa) in MCF10A-M2 cells (Appendix Fig S4A) or using a lentiviral ectopic expression construct in A549 cells (Appendix Fig S4B). TGF- β -induced the downregulation of E-cadherin expression and the upregulation of mesenchymal marker expression were alleviated upon *LITATS1* ectopic expression in both cell lines (Figs 3A and EV2A). On the contrary, *LITATS1* knockdown by two independent shRNA constructs (sh*LITATS1* #1 and #2) enhanced TGF- β -induced expression of two mesenchymal markers in MCF10A-M2 cells (Figs 3B and EV2B). The inhibitory role of *LITATS1* in EMT was also validated in A549 cells via transcriptional profiling and gene set enrichment analysis (GSEA) upon depletion of *LITATS1*. A significant reverse correlation was observed between *LITATS1* expression and a well-

established EMT signature (Fig EV2C). Additionally, *LITATS1* depletion facilitated F-actin formation in the absence of TGF- β and further potentiated TGF- β -induced F-actin formation (Fig 3C). Consistent with these results, *LITATS1* ectopic expression suppressed TGF- β -induced cell migration in MDA-MB-231 and A549 cells, as measured by a chemotactic migration assay (Figs 3D and EV2D). By contrast, *LITATS1* depletion in MDA-MB-231 cells augmented TGF- β -induced cell migration (Fig 3E). In agreement with our *in vitro* migration results, the inhibitory effect of *LITATS1* on cell extravasation was observed in a zebrafish embryo breast cancer xenograft model (Figs 3F and G, and EV2E). Taken together, these data indicate that *LITATS1* functions as a critical suppressor of TGF- β -induced EMT and cell migration.

LITATS1 attenuates TGF- β /SMAD signaling

Next, we investigated the mechanism by which *LITATS1* affects TGF- β -induced EMT and migration. Given that *ZC3H12A* is a head-to-head neighboring gene of *LITATS1* (Fig 1G), we checked the effect of *LITATS1* misexpression on *ZC3H12A* expression. Of note, *ZC3H12A* mRNA expression remained unchanged upon genetic perturbations of *LITATS1* (Appendix Fig S4A–E). Therefore, to explore the signaling pathways affected by *LITATS1* in an unbiased manner, transcriptome analysis of A549 cells with *LITATS1* depletion was carried out (Appendix Fig S5A). Strikingly, 11 of the 15 genes with the greatest upregulation upon *LITATS1* knockdown were bona fide TGF- β /SMAD target genes (fold change > 1.5, $P < 0.05$; Appendix Fig S5B). Furthermore, SMAD3 and SMAD4 were among the top enriched transcription factors that contribute to the gene transcription events mediated by *LITATS1* depletion (Appendix Fig S5C). Pathway enrichment analysis showed that TGF- β signaling was the fourth top pathway among the 10 significantly affected pathways by *LITATS1* depletion (Appendix Fig S5D). In addition, GSEA confirmed the positive correlations between *LITATS1* depletion and the TGF- β gene response signature (Padua *et al*, 2008; Fig 4A). Next, we evaluated the effect of *LITATS1* on TGF- β /SMAD signal transduction using a highly selective synthetic SMAD3/4-driven transcriptional reporter (Dennler *et al*, 1998). *LITATS1* overexpression suppressed, but *LITATS1* depletion potentiated the TGF- β /SMAD3/4-induced transcriptional response in HepG2 cells (Figs 4B and EV3A).

Figure 3. *LITATS1* knockdown potentiates EMT, cell migration, and cell extravasation.

- A, B Effect of *LITATS1* on TGF- β -induced EMT marker expression in MCF10A-M2 upon CRISPRa-mediated *LITATS1* overexpression (A) or shRNA-mediated knockdown (B). GAPDH or α/β -Tubulin, loading control. The results of *LITATS1* overexpression and knockdown are shown in Appendix Fig S4A and Fig EV2B. Representative results from a minimum of three independent experiments are shown.
- C Immunofluorescence analysis of F-actin expression and localization in A549 cells upon shRNA-mediated *LITATS1* depletion. Cells were treated with or without TGF- β for 24 h. Nuclei were visualized by DAPI staining. Scale bar = 30 μ m. The result of *LITATS1* knockdown is shown in Appendix Fig S4C. Representative results from two independent experiments are shown.
- D, E An IncuCyte chemotactic migration assay was performed to evaluate the effect of *LITATS1* ectopic expression (D) or knockdown (E) on TGF- β -induced MDA-MB-231 cell migration. The results of *LITATS1* overexpression and knockdown are shown in Appendix Fig S4D and E. Representative results from two independent experiments are shown.
- F, G *In vivo* zebrafish extravasation experiments with MDA-MB-231 cells upon ectopic *LITATS1* expression (F) or *LITATS1* knockdown (G). Representative zoomed images of the tail fin area are shown in the left panels. Extravasated breast cancer cell clusters are indicated with yellow arrows. Analysis of the extravasated cell cluster numbers in the indicated groups is shown in the right panels. Whole zebrafish image, bar = 309.4 μ m; zoomed image, bar = 154.7 μ m. Representative results from two independent experiments are shown.

Data information: TGF- β was applied at a final concentration of 1 ng/ml. (D, E) are expressed as the mean \pm SD values from four biological replicates ($n = 4$). (F, G) are expressed as the mean \pm SD values from 30 biological replicates ($n = 30$). * $0.01 < P < 0.05$; *** $0.0001 < P < 0.001$; **** $P < 0.0001$. In (D, E), statistical analysis was based on two-way ANOVA. In (F, G), statistical analysis was based on the unpaired Student's *t*-test.

Source data are available online for this figure.

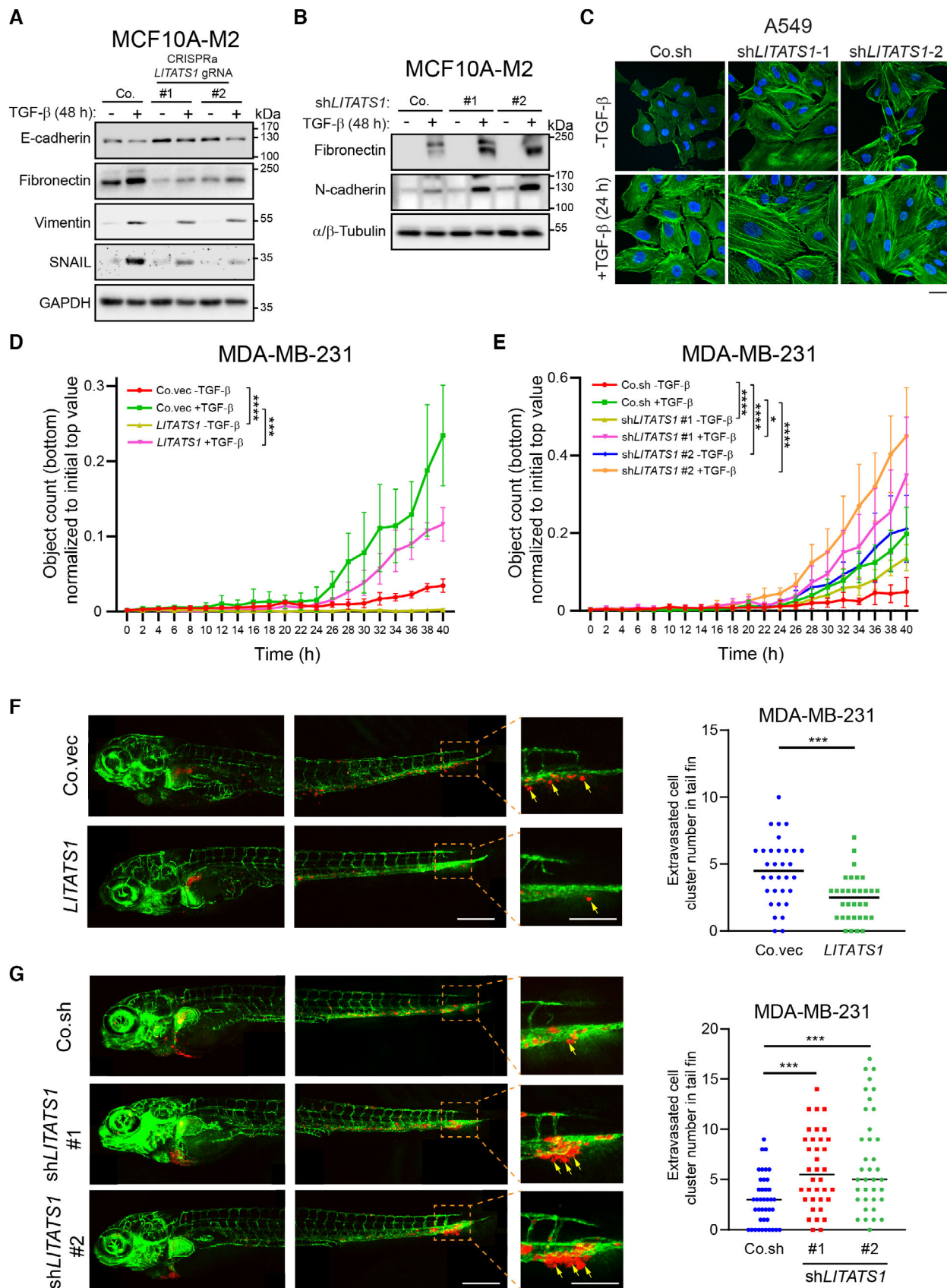


Figure 3.

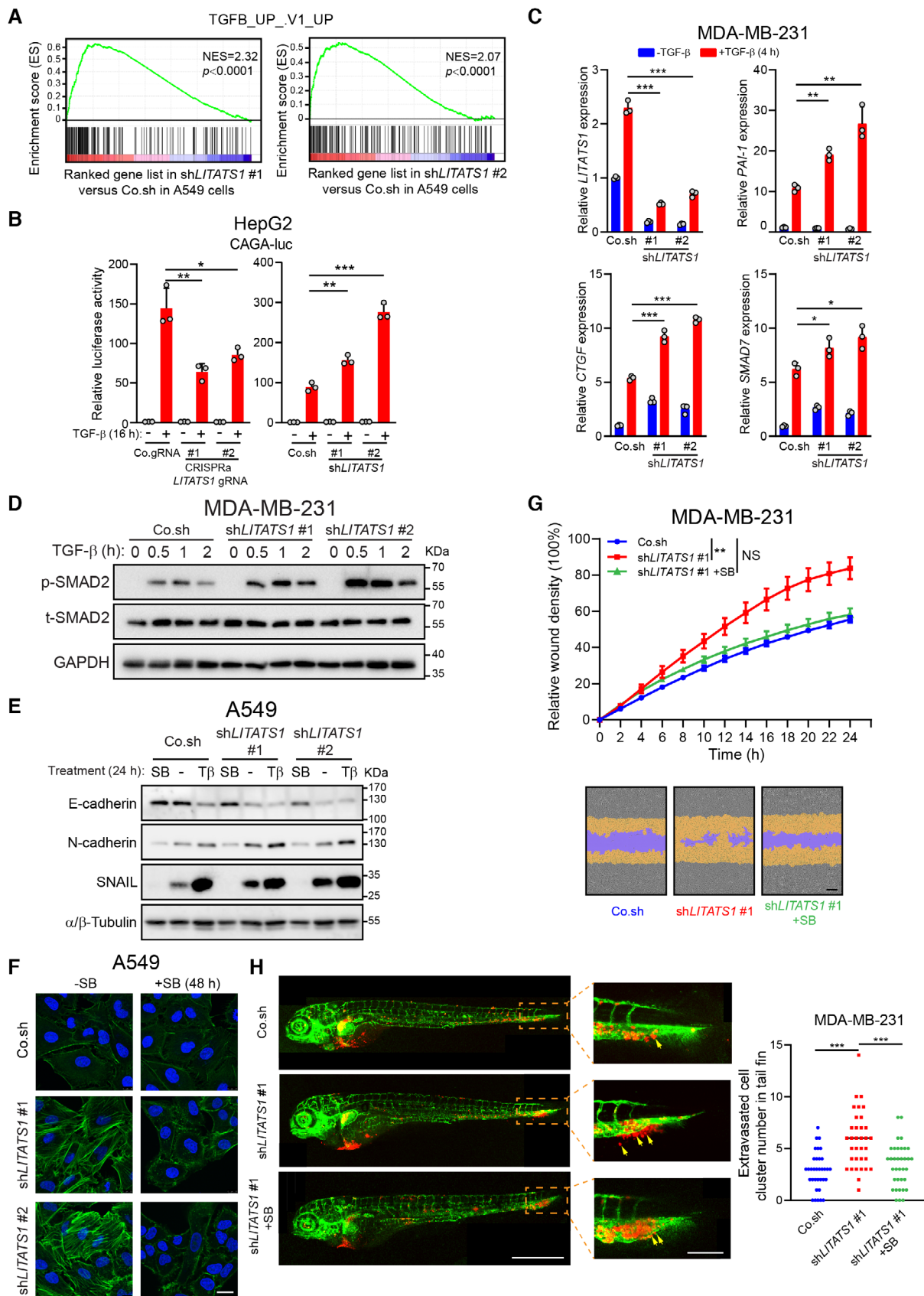


Figure 4.

Figure 4. *LITATS1* suppresses TGF- β /SMAD signaling and EMT.

- A GSEA of positive correlations between (manipulated) *LITATS1* expression and the TGF- β gene response signature.
- B Effect of *LITATS1* misexpression on TGF- β /SMAD3 transcriptional activity in HepG2 cells. Cells were transfected with expression constructs for the TGF- β -induced SMAD3/4-dependent CAGA-luc transcriptional reporter and the *LITATS1* misexpression construct. The results of *LITATS1* misexpression are shown in Fig EV3A. Representative results from a minimum of three independent experiments are shown.
- C Expression of TGF- β target genes (as measured by RT-qPCR) in MDA-MB-231 cells without (Co.sh) or with (sh#1 and sh#2) *LITATS1* depletion. Cells were serum starved for 16 h and treated with or without TGF- β for 4 h. Representative results from a minimum of three independent experiments are shown.
- D Effect of *LITATS1* knockdown on TGF- β -induced SMAD2 phosphorylation in MDA-MB-231 cells. Cells were serum starved for 16 h and stimulated with TGF- β for the indicated durations. The p-SMAD2 and total SMAD2 (t-SMAD2) levels were analyzed by western blotting. GAPDH, loading control. Representative results from a minimum of three independent experiments are shown.
- E Effect of *LITATS1* knockdown on E-cadherin, N-cadherin, and SNAIL expression in A549 cells. Cells were stimulated with vehicle control (–), SB431542 (SB; 10 μ M), or TGF- β (T β) for 24 h, and protein expression was analyzed by western blotting. α / β -Tubulin, loading control. Representative results from a minimum of three independent experiments are shown.
- F Effect of *LITATS1* depletion (using two independent shRNAs, i.e., sh*LITATS1* #1 and #2) on F-actin expression and localization (as evaluated by immunofluorescence) in A549 cells. DAPI staining was performed to visualize nuclei. Cells were stimulated with or without SB431542 (SB; 10 μ M) for 48 h. Scale bar = 30 μ m. Representative results from two independent experiments are shown.
- G IncuCyte wound healing migration assays were performed to evaluate the effect of TGF- β signaling inactivation on MDA-MB-231 cell migration mediated by *LITATS1* knockdown. Cells were treated with or without SB431542 (SB; 10 μ M) during the migration assays. Representative results from two independent experiments are shown.
- H *In vivo* zebrafish extravasation experiments with MDA-MB-231 cells upon *LITATS1* knockdown and blockage of TGF- β signaling. Representative zoomed images of the tail fin area are shown in the left panels. Extravasated breast cancer cell clusters are indicated with yellow arrows. Analysis of the extravasated cell cluster numbers in the indicated groups is shown in the right panel. Whole zebrafish image, bar = 618.8 μ m; zoomed image, scale bar = 154.7 μ m. Representative results from two independent experiments are shown.

Data information: TGF- β was applied at a final concentration of 1 ng/ml. (B, C) are expressed as the mean \pm SD values from three biological replicates ($n = 3$). (C) is expressed as the mean \pm SD from seven biological replicates ($n = 7$). (H) is expressed as the mean \pm SD values from 30 biological replicates ($n = 30$). * $0.01 < P < 0.05$; ** $0.001 < P < 0.01$; *** $0.0001 < P < 0.001$; NS, not significant. In (B, C, H), statistical analysis was based on the unpaired Student's *t*-test. In (G), statistical analysis was based on two-way ANOVA followed by Tukey's multiple comparisons test. Source data are available online for this figure.

Notably, a *LITATS1* mutant (MUT) in which all the putative start codons were mutated (ATG to ATT) exhibited an inhibitory effect on the TGF- β /SMAD3/4-induced transcriptional response similar to that of wild-type (WT) *LITATS1* (Fig EV3B). This finding was consistent with the prediction of *LITATS1* to be a lncRNA that does not encode small peptides despite its cytoplasmic localization. Moreover, *LITATS1* knockdown promoted the expression of TGF- β /SMAD target genes in MDA-MB-231 and MCF10A-M2 cells (Figs 4C and EV3C). By contrast, *LITATS1* overexpression attenuated TGF- β /SMAD-induced target gene expression in both cell lines (Fig EV3D and E). Furthermore, TGF- β -induced SMAD2 phosphorylation, which is an immediate downstream indicator of T β RI activity, was promoted in MDA-MB-231 and MCF10A-M2 cells with *LITATS1* depletion (Figs 4D and EV3F). However, TGF- β -induced SMAD2 phosphorylation was mitigated upon ectopic *LITATS1* expression in MDA-MB-231 and MCF10A-M2 cells (Fig EV3G–I). Moreover, the negative regulatory effect of *LITATS1* on TGF- β /SMAD signaling was confirmed by *LITATS1* misexpression in A549 cells (Appendix Fig S5E–G).

We then determined whether the effect of *LITATS1* on uncontrolled EMT is dependent on TGF- β signaling regulation. The *LITATS1* depletion-mediated changes in EMT marker expression and F-actin formation were mitigated by blockade of TGF- β /SMAD signaling with the selective T β RI kinase inhibitor SB431542 in A549 cells (Fig 4E and F, Appendix Fig S5H). Moreover, SB431542 treatment blocked the migration of MDA-MB-231, MCF10A-M2, and A549 cells and the *in vivo* extravasation of MDA-MB-231 cells that were induced by *LITATS1* knockdown (Figs 4G and H, and EV3J, Appendix Fig S5I). Taken together, these results indicate that TGF- β receptor signaling activation is pivotal for the promoting effects on EMT, cell migration, and extravasation that occur upon *LITATS1* depletion.

***LITATS1* destabilizes T β RI by potentiating its polyubiquitination**

The promotion of T β RI-induced SMAD2 phosphorylation resulting from the absence of *LITATS1* (Fig 4D) prompted us to check whether *LITATS1* affects the expression of its upstream TGF- β receptor. We found that upon *LITATS1* ectopic expression, MDA-MB-231 and MCF10A-M2 cells exhibited less T β RI protein expression (Figs 5A and EV4A). This was further confirmed by ectopic expression of *LITATS1* in caT β RI-overexpressing HEK293T cells (Fig EV4B). Interestingly, *TBRI* mRNA expression remained unaffected (Fig EV4A and C). Consistent with these results, depletion of *LITATS1* enhanced T β RI expression at the protein but not at the mRNA level (Figs 5B and EV4C and D). These results suggest that *LITATS1* may alter T β RI protein turnover. Consistent with this idea, *LITATS1* exerted a negative effect on T β RI protein stability, as measured by a cycloheximide (CHX)-directed time-course assay (Figs 5C and D, and EV4E). To decipher whether lysosomes or proteasomes play a role in the inhibitory effect of *LITATS1* on T β RI protein stability, *LITATS1*-overexpressing MDA-MB-231, and HEK293T cells were challenged with selective chemical lysosome or proteasome inhibitors. *LITATS1*-induced T β RI downregulation was restored only by the proteasome inhibitor MG132 but not by either of the two tested lysosome inhibitors (bafilomycin A1 (BafA1) and hydroxychloroquine (HCQ); Figs 5E and EV4F). Consistent with these results, ectopic *LITATS1* expression greatly increased the T β RI polyubiquitination level (Fig 5F). In addition, *TBRI* knockdown alleviated the induction of EMT resulting from *LITATS1* knockdown in A549 cells (Fig EV4G), suggesting that T β RI is an indispensable target of *LITATS1* in its regulation of EMT. Taken together, these results indicate that *LITATS1* potentiates T β RI polyubiquitination and degradation.

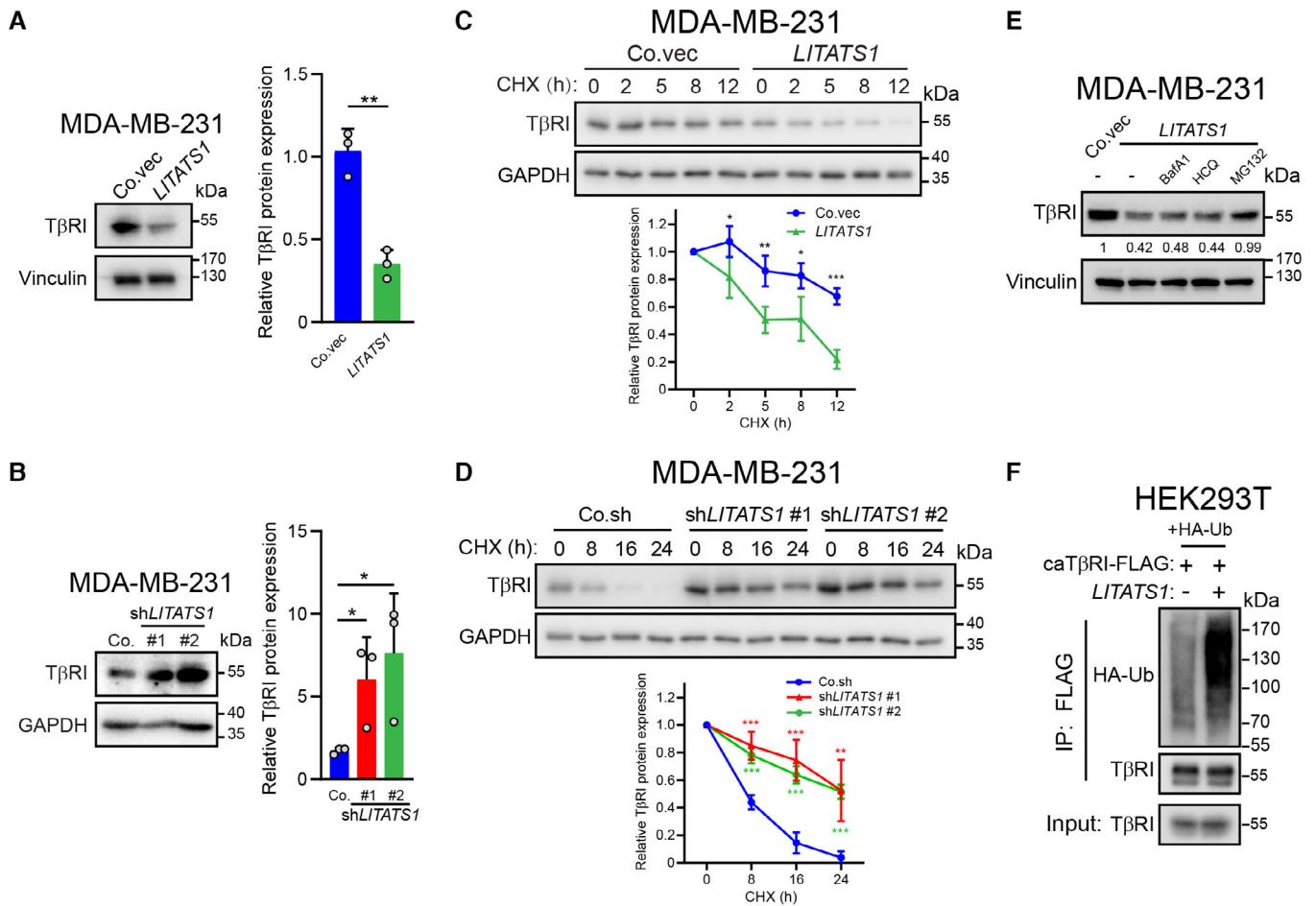


Figure 5. *LITATS1* promotes the ubiquitination and degradation of $T\beta$ RI.

A, B Effect of ectopic *LITATS1* expression (A) or *LITATS1* knockdown (B) on $T\beta$ RI expression in MDA-MB-231 cells. Right panel: quantification of relative $T\beta$ RI protein levels. Vinculin or GAPDH, loading control. Representative blots from a minimum of three independent experiments are shown.

C, D Analysis of $T\beta$ RI protein stability (as measured by western blotting) in MDA-MB-231 cells with ectopic *LITATS1* expression (C) or *LITATS1* knockdown (D). Cells were treated with CHX (50 μ g/ml) for the indicated durations. Quantification of the relative $T\beta$ RI protein level is shown in the lower panels. GAPDH, loading control. Representative blots from a minimum of three independent experiments are shown.

E $T\beta$ RI expression in MDA-MB-231 cells with ectopic *LITATS1* expression in the absence or presence of lysosome or proteasome inhibitors. Cells were incubated with vehicle control DMSO (–), the lysosome inhibitor BafA1 (20 nM) or HCQ (20 μ M), or the proteasome inhibitor MG132 (5 μ M) for 8 h. Vinculin, loading control. Representative results from a minimum of three independent experiments are shown.

F Effect of *LITATS1* on $T\beta$ RI polyubiquitination. HEK293T cells were transfected with ectopic expression constructs for HA-Ubiquitin (HA-Ub), ca $T\beta$ RI-FLAG, and/or *LITATS1*. $T\beta$ RI polyubiquitination was analyzed by western blotting. Representative blots from a minimum of three independent experiments are shown.

Data information: (A, B) are expressed as the mean \pm SD values from three biological replicates ($n = 3$). (C, D) are expressed as the mean \pm SD values from four biological replicates ($n = 4$). * $0.01 < P < 0.05$; ** $0.001 < P < 0.01$; *** $0.0001 < P < 0.001$. Statistical analysis was based on the unpaired Student's *t*-test. Source data are available online for this figure.

LITATS1 interacts with $T\beta$ RI and SMURF2

To reveal the mechanism by which *LITATS1* increases $T\beta$ RI polyubiquitination, RNA immunoprecipitation (RIP) coupled with RT-qPCR was performed on lysates from HEK293T cells with ectopic expression of different FLAG-tagged TGF- β /SMAD signaling components (i.e., SMAD2, SMAD3, SMAD4, and $T\beta$ RI) or modulators (i.e., SMAD7 and the E3 ubiquitin ligases SMURF1/2). Notably, only ca $T\beta$ RI and SMURF2 but not the other ectopically expressed proteins, were capable of coprecipitating *LITATS1* (Figs 6A and EV5A). A recently developed CRISPR-assisted RNA-protein interaction

detection method (CARPID; Yi *et al*, 2020), which incorporates CRISPR-CasRx-mediated RNA targeting and proximity labeling to verify endogenous interactions between lncRNAs and proteins of interest, was utilized to validate the interaction between *LITATS1* and $T\beta$ RI or SMURF2. The specific sequence-matching gRNAs can direct the TurboID-dCasRx complex to *LITATS1*, where RNA-binding proteins in close proximity to *LITATS1* can be labeled with biotin and analyzed by western blotting after enrichment with streptavidin beads (Fig EV5B). We selected the two most effective gRNAs (gRNA #1 and #2) based on the CasRx-directed degradation of *LITATS1* as measured by RT-qPCR (Fig EV5C). As expected,

overexpression of these two independent gRNAs increased the biotinylation level of SMURF2 and TβRI in MDA-MB-231 cells (Fig 6B). This effect was further enhanced in the presence of TGF-β and was likely mediated by TGF-β-induced *LITATS1* expression. We further confirmed the interactions between *LITATS1* and TβRI or SMURF2 at the endogenous level in MDA-MB-231 cells using RIP analysis (Fig 6C). When we checked TGF-β-induced *LITATS1* expression, we

observed that TGF-β stimulation could not further enhance the interactions between *LITATS1* and TβRI or SMURF2 (Figs EV5D and 5E). To orthogonally confirm these findings, we performed RNA pull-down assays using biotinylated *LITATS1* and negative controls, including biotinylated antisense *LITATS1* and 25× poly(A), and proteins produced from HEK293T cells. Western blot analysis revealed that *LITATS1* bound to caTβRI and SMURF2 proteins (Fig 6D).

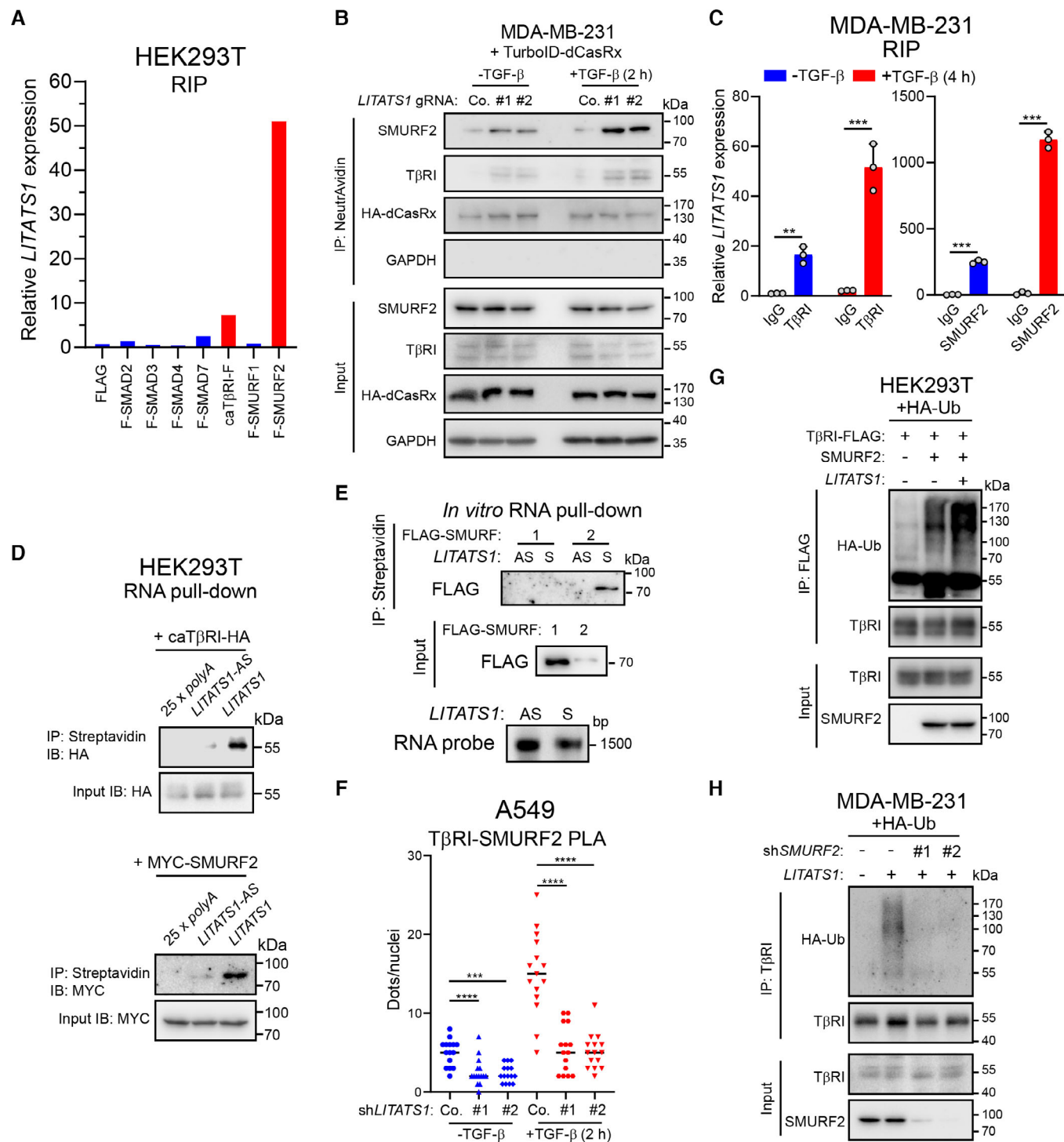


Figure 6.

Figure 6. *LITATS1* interacts with TβRI and SMURF2.

- A Interactions between *LITATS1* and TGF-β/SMAD signaling components or modulators were analyzed by RIP. RT-qPCR was performed to detect *LITATS1* expression in immunoprecipitates from HEK293T cells transfected with expression constructs for the indicated proteins. Representative results from two independent experiments are shown.
- B Interactions between *LITATS1* and TβRI or SMURF2 in MDA-MB-231 cells were detected by the CARPID approach. Cells with stable expression of TurboID-dCasRx were transduced without (Co.) or with (#1 and #2) *LITATS1* targeting gRNAs. Cells were stimulated with or without TGF-β (2.5 ng/ml) for 2 h and were then stimulated with biotin (500 μM) for 30 min. Western blotting was performed to detect SMURF2 and TβRI expression in whole-cell lysates (Input) and immunoprecipitates (IP). GAPDH and HA-dCasRx expression levels were measured for equal loading of Input samples and as the negative control or positive control, respectively, for proximity biotinylation in immunoprecipitate (IP) samples. Representative results from a minimum of three independent experiments are shown.
- C Interactions between *LITATS1* and TβRI (left) or SMURF2 (right) were analyzed by RIP. MDA-MB-231 cells were stimulated with or without TGF-β (5 ng/ml) for 4 h before RIP. RT-qPCR was performed to detect *LITATS1* expression in immunoprecipitates from MDA-MB-231 cells. IgG was included as the control for immunoprecipitation. Representative results from two independent experiments are shown.
- D Interactions between *LITATS1* and caTβRI or SMURF2 were analyzed by RNA pull-down. Biotinylated 25x poly(A), antisense *LITATS1* (*LITATS1-AS*), or *LITATS1* was incubated with lysates from HEK293T cells transfected with the caTβRI-HA or MYC-SMURF2 expression construct. Western blot analysis was performed to detect HA or MYC expression in whole-cell lysates (Input) and immunoprecipitates (IP). Representative blots from a minimum of three independent experiments are shown.
- E *In vitro* RNA pull-down assays were performed to evaluate the interactions between *LITATS1* and SMURF1/2. *In vitro*-transcribed antisense *LITATS1* (*LITATS1-AS*) or *LITATS1* (*LITATS1-S*) was incubated with recombinant FLAG-tagged SMURF1 or SMURF2 protein. Western blotting analysis was performed to evaluate FLAG expression in input and IP samples. The amounts of RNA probes used for RNA pull-down were evaluated by agarose gel electrophoresis. Representative results from a minimum of three independent experiments are shown.
- F Quantification of TβRI-SMURF2 PLA in A549 cells with or without *LITATS1* knockdown were treated with or without TGF-β (5 ng/ml) for 2 h. Representative images are shown in Fig EV5F.
- G Effect of *LITATS1* overexpression on SMURF2-mediated TβRI polyubiquitination. HEK293T cells were transfected with expression constructs for HA-Ubiquitin (HA-Ub) and caTβRI-FLAG and ectopic expression constructs for SMURF2 and/or *LITATS1*. Polyubiquitination of TβRI was evaluated by western blotting. Representative blots from a minimum of three independent experiments are shown.
- H Effect of *SMURF2* knockdown on *LITATS1*-mediated TβRI polyubiquitination. MDA-MB-231 cells with stable HA-Ub expression were transduced with expression constructs for *LITATS1* and/or two different *SMURF2* shRNAs, as indicated. Polyubiquitination of TβRI was evaluated by western blotting. Representative blots from a minimum of three independent experiments are shown.

Data information: (C) is expressed as the mean ± SD values from three ($n = 3$) biological replicates. (F) is expressed as the mean values from 15 ($n = 15$) biological replicates. **0.001 < $P < 0.01$; ***0.0001 < $P < 0.001$; **** $P < 0.0001$. Statistical analysis was based on the unpaired Student's t -test. Source data are available online for this figure.

In vitro RIP analysis using *in vitro*-transcribed *LITATS1* and the recombinant protein of TβRI intracellular domain (ICD) further confirmed the direct interaction between *LITATS1* and TβRI (Appendix Fig S6A). Moreover, *in vitro* RNA pull-down showed that recombinant SMURF2 but not its homologous protein SMURF1 could coprecipitate with *LITATS1* (Fig 6E). Given that SMURF2 can be recruited to TβRI with the aid of SMAD7, thereby promoting TβRI polyubiquitination and degradation (Kavsak *et al*, 2000), we reasoned that *LITATS1* may also serve as a scaffold to potentiate SMURF2-TβRI interaction. The results of the proximity ligation assay (PLA) in A549 cells demonstrated that TGF-β stimulation resulted in a three-fold increase of SMURF2-TβRI interaction, which was mitigated upon *LITATS1* knockdown (Figs 6F and EV5F). Of note, we found a moderate induction of *LITATS1* (1.7-fold increase) upon 2 h TGF-β stimulation in the RNA-seq analysis of A549 cells, indicating that *LITATS1* promotes TβRI-SMUR2 interaction also independent from its induction by TGF-β, likely by acting as a scaffold. Furthermore, ectopic *LITATS1* expression enhanced SMURF2-induced TβRI polyubiquitination (Fig 6G). Importantly, SMURF2 depletion markedly diminished the increase in TβRI polyubiquitination induced by ectopic *LITATS1* expression (Fig 6H). This latter result indicates that SMURF2 is a key E3 ubiquitin ligase partner of *LITATS1* by which it mediates TβRI polyubiquitination.

***LITATS1* binds to the WW1 domain of SMURF2 and promotes the cytoplasmic retention of SMURF2**

To map the SMURF2 binding region in *LITATS1*, interactions between SMURF2 and full-length *LITATS1* (Appendix Fig S6B) or four RNA fragments, each representing approximately one-fourth

of the *LITATS1* sequence, were evaluated by RNA pull-down (Appendix Fig S6C-F). We observed an interaction between SMURF2 and only the *LITATS1* 5' fragment (T1; 1-350 nt), although this binding was impaired compared with that between SMURF2 and full-length *LITATS1* (Fig 7A). Moreover, analysis of the binding capability of *LITATS1* to SMURF2 truncation mutants demonstrated that the WW1 domain, which is not present in SMURF1, was essential for the binding of SMURF2 to *LITATS1* (Fig 7B-D).

As SMURF2 is translocated from the nucleus to the cytoplasm in response to TGF-β (Kavsak *et al*, 2000) via a not well-characterized mechanism, we next investigated whether cytoplasmic *LITATS1* alters the subcellular distribution of SMURF2. The immunofluorescence results revealed that *LITATS1* depletion decreased the proportion of cytoplasmic SMURF2 in A549 cells (Fig 7E). Additionally, subcellular fractionation confirmed the attenuation of SMURF2 cytoplasmic localization upon the loss of *LITATS1* (Fig 7F). Consistent with these results, more SMURF2 was retained in the cytoplasm in *LITATS1*-overexpressing MDA-MB-231 cells (Appendix Fig S6G). Of note, SMURF2 protein expression was not affected upon *LITATS1* knockdown (Appendix Fig S6H). Taken together, these results indicate that *LITATS1* potentiates the cytoplasmic retention of SMURF2 without affecting its expression.

Discussion

In this study, we identified *LITATS1* as a critical determinant of epithelial integrity maintenance and inhibitor of TGF-β-induced EMT in breast and non-small cell lung cancer cells. *LITATS1* suppresses

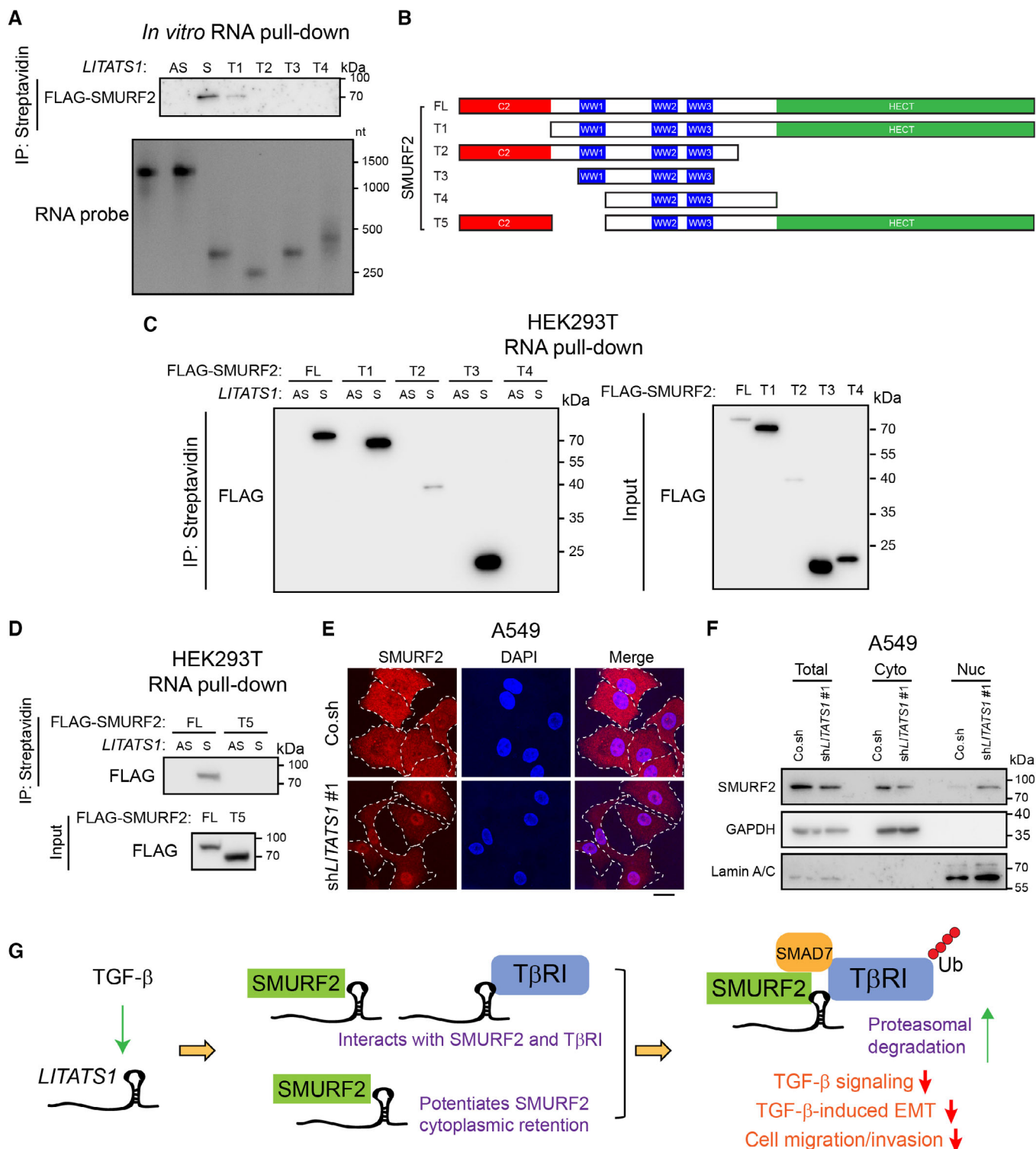


Figure 7.

TGF- β /SMAD signaling by interacting with SMURF2 and T β RI and promoting the cytoplasmic retention of SMURF2. T β RI polyubiquitination and proteasomal degradation are potentiated by *LITATS1*, leading to suppression of TGF- β /SMAD signaling, TGF- β -induced EMT, and cell migration/invasion (Fig 7G).

We showed that *LITATS1* is the only *ZC3H12A-DT* splice variant that can be induced by TGF- β in breast and non-small cell lung cancer cell lines. To further exclude the involvement of the other six splice variants in the *LITATS1*-mediated effects, we checked the sequences of *LITATS1*-targeting shRNAs and GapmeRs (Appendix

Figure 7. *LITATS1* retains SMURF2 in the cytoplasm.

- A An *in vitro* RNA pull-down assay was performed to evaluate the interaction between *LITATS1* truncation mutants and SMURF2. Recombinant FLAG-SMURF2 protein was incubated with antisense *LITATS1* (*LITATS1*-AS), *LITATS1* (*LITATS1*-S), or *LITATS1* truncation mutants (T1-T4). Western blot analysis was performed to evaluate FLAG expression in immunoprecipitates (IP). The amounts of RNA probes used for RNA pull-down were evaluated by agarose gel electrophoresis. Representative results from a minimum of three independent experiments are shown.
- B Schematic representation of full-length SMURF2 (FL) and the truncation mutants (T1-T5) tested.
- C, D RNA pull-down assays were performed to evaluate the interaction between *LITATS1* and full-length SMURF2 or its truncation mutants (T1-T5) expressed in HEK293T cells. Western blotting analysis was performed to evaluate FLAG expression in input and immunoprecipitate (IP) samples. Representative results from a minimum of three independent experiments are shown.
- E SMURF2 expression and localization (as measured by immunofluorescence) upon *LITATS1* depletion in A549 cells. DAPI staining was performed to visualize nuclei. Scale bar = 23.2 μ m. Representative results from two independent experiments are shown.
- F Effect of *LITATS1* knockdown on SMURF2 localization in A549 cells. After subcellular protein fractionation, western blotting was performed to detect SMURF2 expression in whole-cell lysates (Total) and the cytoplasmic (Cyto) and nuclear (Nuc) fractions. The levels of the cytoplasmic marker GAPDH and the nuclear marker Lamin A/C are included to demonstrate subcellular protein fractionation. Representative results from two independent experiments are shown.
- G Schematic working model. TGF- β -induced *LITATS1* interacts with T β RI and SMURF2 and potentiates cytoplasmic retention of SMURF2. The expression of *LITATS1* potentiates T β RI polyubiquitination and proteasomal degradation, resulting in suppression of TGF- β signaling, TGF- β -induced EMT, and cancer cell migration/invasion.

Source data are available online for this figure.

Fig S3A). ShRNA #2 and two GapmeRs target the exon 4 that is shared by variants 1, 4, 5, and 6, while shRNA #1 can specifically target the exon 3, which exists only in *LITATS1*. Consistent with the results that *LITATS1* is the main TGF- β -induced *ZC3H12A-DT* splice variant, shRNA #1-mediated *LITATS1* knockdown affected TGF- β -induced EMT as potent as shRNA #2 and two GapmeRs (Fig 3B and C, and Appendix Fig S2C and D). In addition, the effects of both shRNA constructs on TGF- β signaling regulation are similar (Figs 4 and 5). These results suggest that *LITATS1* is the only *ZC3H12A-DT* splice variant that plays a role in our study.

TGF- β /SMAD-induced *LITATS1* mitigates T β RI protein turnover and thereby suppresses TGF- β /SMAD signal transduction. Frequently, the products of genes that are transcriptionally induced by TGF- β act in negative or positive feedback loops to fine-tune the intensity and/or duration of TGF- β signaling responses (Nakao *et al*, 1997; Kang *et al*, 2003) or participate as effectors in TGF- β -induced biological impacts (Massague & Gomis, 2006; Katsuno *et al*, 2013). These scenarios also apply to lncRNAs. TGF- β signaling can induce the expression of multiple lncRNAs, e.g., *lncRNA-ATB* and *lncRNA-HIT*, which function as effectors of TGF- β -induced responses (Yuan *et al*, 2014; Richards *et al*, 2015). In addition, certain lncRNAs can act as modulators of TGF- β signaling by altering the expression or activity of TGF- β signaling components (Wang *et al*, 2018; Papoutsoglou *et al*, 2019; Sakai *et al*, 2019; Papoutsoglou & Moustakas, 2020; Xu *et al*, 2021). Several lines of evidence indicate that *TBR1* mRNA expression is regulated by lncRNAs at both the transcriptional (Xu *et al*, 2021) and post-transcriptional (Li *et al*, 2018, 2021; Zhou *et al*, 2018; Jin *et al*, 2020; Yang & Lin, 2020; Cheng *et al*, 2021; Hu *et al*, 2021; Qi *et al*, 2021; Zhu *et al*, 2022) levels. However, our results reveal a novel mechanism by which T β RI protein stability is modulated through lncRNA-mediated post-translational modification. LncRNAs have been reported to modulate protein polyubiquitination. Vimentin-associated lncRNA (*VAL*) binds to Vimentin and abrogates Trim16-mediated Vimentin polyubiquitination (Tian *et al*, 2020). In senescent cells, *HOTAIR* facilitates the polyubiquitination of Ataxin-1 and Dzip3 by promoting their associations with the E3 ligases Snurportin-1 and Mex3b, respectively (Yoon *et al*, 2013). For *LITATS1*, SMURF2 appears to be necessary to potentiate T β RI polyubiquitination. However, the contributions of other E3 ligases to this process cannot be excluded.

We mapped the binding region of SMURF2 in the 5' fragment of *LITATS1* (*LITATS1*-T1) by analyzing the *LITATS1* truncation mutants. However, SMURF2 could not interact as potently with *LITATS1*-T1 as full-length *LITATS1*. Considering the importance of lncRNA folding structure for its interactions with proteins (Hu *et al*, 2018; Sanchez de Groot *et al*, 2019), it is highly possible that *LITATS1* truncation may impair its original folding structure that is required for SMURF2 binding. Therefore, checking interactions between SMURF2 and *LITATS1* mutants with small deletions or nucleotide substitutions that elicit minimal effects on *LITATS1* folding can better explore the SMURF2 binding region in *LITATS1*. Moreover, other approaches such as cross-linking and immunoprecipitation (CLIP) coupled with RNA footprinting (Kishore *et al*, 2011) can be applied to identify the binding sites of SMURF2 or T β RI in *LITATS1* in live cells.

In response to TGF- β stimulation, SMAD7 binds SMURF2 to activate the ubiquitin ligase activity of SMURF2 by suppressing its auto-inhibition and recruits SMURF2 to target T β RI for degradation (Kavsak *et al*, 2000; Budi *et al*, 2017). Similar to SMAD7, *LITATS1* may serve as a scaffold to facilitate the T β RI-SMURF2 interaction. However, we found that *SMAD7* knockdown mitigated *LITATS1*-directed polyubiquitination of T β RI (Appendix Fig S6I), demonstrating that SMAD7 is required for *LITATS1* to exert its effect on T β RI. Our RIP results suggested a weak interaction between SMAD7 and *LITATS1* (Fig 6A) that is less potent than the interactions between *LITATS1* and T β RI/SMURF2. These results can be explained by the possibility that *LITATS1* is a component of the T β RI/SMURF2/SMAD7 complex and therefore indirectly binds SMAD7. However, *SMAD7* knockdown does not affect the interaction between *LITATS1* and T β RI, indicating that the binding of *LITATS1* to T β RI is SMAD7-independent (Appendix Fig S6J). Therefore, further study is required to investigate whether SMAD7 and *LITATS1* function in an additive manner to facilitate the SMURF2/T β RI complex formation.

We observed a significant decrease in *LITATS1* expression in lung adenocarcinoma tissues and mesenchymal breast cancer cells. Moreover, *LITATS1* is localized in the cytoplasm, and its expression can be induced by TGF- β . The remaining question is how *LITATS1* expression is modulated at other levels during cancer progression. Tumor-inhibitory miR-22-3p was identified as an upstream modulator of *LITATS1* expression in oral squamous cell carcinoma cells

(Du et al, 2021). Thus, specific tumor-promoting miRNAs may target *LITATS1* for degradation in breast cancer and lung cancer progression. Moreover, *LITATS1* was shown to be a short-lived lncRNA that is degraded by nuclear RNases in HepG2 cells (Tani et al, 2019). Therefore, certain cancer-related cytoplasmic RNases or RNA-binding proteins may alter *LITATS1* stability. Additionally, we could not rule out the possibility that *LITATS1* expression is changed by epigenetic modifications such as promoter hypermethylation.

Our results showed that higher *LITATS1* expression correlates with a favorable survival outcome in breast and non-small cell lung cancer patients. These results highlight the predictive potential of *LITATS1* expression for cancer progression. Given their cell/tissue-specific expression pattern and dysregulation during cancer progression, lncRNAs are emerging as effective biomarkers for cancers (Beylerli et al, 2022). For example, the urine-based test for the lncRNA *PCA3* has been approved by the FDA for prostate cancer diagnosis (Groskopf et al, 2006) and has been further developed as a promising prognostic marker (Ferro et al, 2015; Cantiello et al, 2016). We also found that reintroducing *LITATS1* into highly aggressive MDA-MB-231 cells impaired their migration and extravasation, indicating that *LITATS1* may be a therapeutic agent for cancers. Hence, RNA delivery systems, such as lipid nanoparticles (LNPs), which have been extensively tested and optimized as carriers of therapeutic mRNA molecules (Lutz et al, 2017; Ickenstein & Garidel, 2019), can be applied to transduce *LITATS1* and evaluate its therapeutic value in preclinical *in vivo* models.

Materials and Methods

Cell culture and reagents

HEK293T (CRL-1573), HepG2 (HB-8065), A549 (CRM-CCL-185), A549 (CCL-185EMT), MDA-MB-231 (CRM-HTB-26), MDA-MB-436 (HTB-130), and MCF7 (HTB-22) cells were purchased from the American Type Culture Collection (ATCC) and cultured in Dulbecco's modified Eagle medium (DMEM; Thermo Fisher Scientific; 41965062) supplemented with 10% fetal bovine serum (FBS; Thermo Fisher Scientific; 16000044) and 100 U/ml penicillin/streptomycin (Thermo Fisher Scientific; 15140163). MCF10A-M1 and MCF10A-M2 cells were kindly provided by Dr. Fred Miller (Barbara Ann Karmanos Cancer Institute, Detroit, USA) and cultured in DMEM/F12 (GlutaMAX™ Supplement; Thermo Fisher Scientific; 31331028) containing 5% horse serum (Thermo Fisher Scientific; 26050088), 0.1 µg/ml cholera toxin (Sigma-Aldrich; C8052), 0.02 µg/ml Epidermal Growth Factor (EGF; Sigma-Aldrich; 01-107), 0.5 µg/ml hydrocortisone (Sigma-Aldrich; H0135), 10 µg/ml insulin (Sigma-Aldrich; I6634), and 100 U/ml penicillin/streptomycin. All cell lines were maintained in a 5% CO₂, 37 °C humidified incubator, tested monthly for mycoplasma contamination, and checked for authenticity by short tandem repeat (STR) profiling. The protein synthesis inhibitor cycloheximide (CHX; Sigma-Aldrich; C1988) was added to the medium at a concentration of 50 µg/ml. Two lysosome inhibitors, BafA1 (Sigma-Aldrich; B1793) and HCQ (Sigma-Aldrich; H0915), were used at final concentrations of 20 nM and 20 µM, respectively. The proteasome inhibitor MG132 (Sigma-Aldrich; 474787) was used at a final concentration of 5 µM. A selective small

molecule kinase inhibitor of TBRI (SB431542; SB; Laping et al, 2002) was used at a concentration of 10 µM. Recombinant TGF-β3 and recombinant BMP6 were kind gifts from Andrew Hinck (University of Pittsburgh) and Slobodan Vukicevic (University of Zagreb, Croatia), respectively.

Plasmid construction

Full-length *LITATS1* was amplified by PCR from MDA-MB-231 cell-derived cDNA and inserted into the lentiviral vector pCDH-EF1α-MCS-polyA-PURO. Two independent shRNAs, CRISPRa gRNAs and CasRx gRNAs were designed and inserted into the lentiviral vectors pLKO.1, lenti sgRNA (MS2)_puro optimized backbone (Addgene; 73797), PLKO.1-U6-PURO (AA19), and pRX004-pregRNA (Addgene; 109054), respectively. *LITATS1* promoter fragments were amplified from MDA-MB-231 genomic DNA and subcloned into the pGL4-luc backbone (Promega). The construct expressing dCasRx-TurboID was modified from a CARPID dCasRx-BASU plasmid (Addgene; 153303) by replacing a fragment expressing *Bacillus subtilis* biotin ligase (BASU) with a fragment expressing TurboID. All plasmids were verified by Sanger sequencing, and the primers used for plasmid construction are listed in Appendix Table S2.

Lentiviral transduction and transfection

To produce lentivirus, packaging plasmids (VSV, gag, and Rev) and expression constructs for cDNAs or shRNAs were cotransfected into HEK293T cells. At 48 h post-transfection, supernatants were collected from HEK293T cells and added to target cells supplemented with the same volume of fresh medium. After 48 h of infection, puromycin (1 µg/ml; Sigma-Aldrich; P9620) was added to the medium to select stable cells. We used TRCN0000040031 for *SMAD4* knockdown, TRCN0000003478 (#1) and TRCN0000010792 (#2) for *SMURF2* knockdown, TRCN0000127698 (#1) and TRCN0000128209 (#2) for *ZC3H12A* knockdown, and TRCN0000039773 for *TBRI* knockdown. For the transfection of GapmeRs (Eurogentec), 1.2×10^5 A549 cells were seeded in wells of a 12-well plate and incubated with the complex formed by Lipofectamine 3000 (Thermo Fisher Scientific; L3000015) and GapmeRs (25 nM at final concentration). Medium was changed after 6 h. RNA and protein samples were collected at 24 h post-transfection. The sequences of GapmeRs are listed in Appendix Table S3. For siRNA transfection, 10 nM nontargeting siRNA (Dharmacon) or SMARTpool siRNA targeting *SMAD7* (Dharmacon; L-020068-00-0005) was transfected into MDA-MB-231 cells at 80% confluence with DharmaFECT transfection reagents. The medium was changed at 24 h post-transfection.

RT-qPCR

A NucleoSpin RNA kit (Macherey Nagel; 740955) was used to isolate total RNA from cells. Then, reverse transcription was carried out with a RevertAid RT Reverse Transcription Kit (Thermo Fisher Scientific; K1691). The indicated genes were amplified using the synthesized cDNA with specific primer pairs, and signals were visualized with a CFX Connect Real-Time PCR Detection System (Bio-Rad). *GAPDH* was used as the reference gene for normalization by the 2^{-ΔΔCt} method. The primer sequences used for RT-qPCR are listed in Appendix Table S4.

Western blotting

RIPA buffer (150 mM sodium chloride, 1.0% Triton-X-100, 0.5% sodium deoxycholate, 0.1% sodium dodecyl sulfate (SDS), and 50 mM Tris-HCl (pH 8.0)) supplemented with complete protease inhibitor cocktail (Roche; 11836153001) was applied to lyse cells. Subsequently, protein concentrations were evaluated with a DC™ protein assay kit (Bio-Rad; 5000111). Next, SDS-polyacrylamide gel electrophoresis (PAGE) was performed, and proteins were then transferred onto a 0.45- μ m polyvinylidene difluoride (PVDF) membrane (Merck Millipore; IPVH00010). Subsequently, the membrane was blocked with 5% nonfat dry milk in Tris-buffered saline (TBS) with 0.1% Tween 20 detergent (TBST) for 1 h at room temperature. After probing the membranes with the corresponding primary and secondary antibodies, images were acquired with a ChemiDoc Imaging System (Bio-Rad). The primary antibodies used for western blotting are listed in Appendix Table S5. Horseradish peroxidase (HRP)-linked anti-mouse IgG (Sigma-Aldrich; NA931V) and anti-rabbit IgG (Cell Signaling; 7074S) were used as secondary antibodies. ImageJ (National Institutes of Health, United States) was used to quantify relative protein expression levels by densitometry.

Transcriptional reporter assays

To quantify SMAD3/4-driven transcriptional CAGA-luc reporter activity, 3×10^5 HepG2 cells were seeded in the wells of a 24-well plate. The next day, 100 ng of the SMAD3/4-driven transcriptional CAGA-luc plasmid (Dennler *et al*, 1998), 80 ng of the β -galactosidase expression construct, and 320 ng of the indicated expression constructs were cotransfected into HepG2 cells using polyethyleneimine (PEI; Polysciences; 23966). After 16 h incubation and serum starvation for 6–8 h, the cells were stimulated with or without TGF- β (1 ng/ml) for 16 h. To measure the activity of the *LITATS1* promoter fragments, 250 ng of the *LITATS1* promoter luciferase reporter was cotransfected with 80 ng of the β -galactosidase expression construct into HepG2 cells in the presence of PEI or into A549 cells by Lipofectamine 3000. After 16 h incubation and serum starvation for 6–8 h, the cells were stimulated with ligand buffer (vehicle control), TGF- β (5 ng/ml), or BMP6 (50 ng/ml) for 16 h. Luciferase activity was measured with the substrate D-luciferin (Promega) and a luminometer (PerkinElmer) and normalized to β -galactosidase activity. All experiments were performed three times, and representative results are shown.

Immunofluorescence staining

To evaluate the expression and localization of SMURF2 (endogenous or MYC-tagged), immunofluorescence staining was performed as previously described (Liu *et al*, 2020). In brief, cells were fixed with 4% paraformaldehyde (PFA) for 20 min and permeabilized with 0.1% Triton-X in PBS for 10 min. Subsequently, 3% bovine serum albumin (BSA) in PBS was added to block nonspecific binding. For detection of SMURF2, cells were incubated first with a primary antibody against SMURF2 (1:100 dilution; Santa Cruz; sc-393848) or MYC (1:100 dilution; Santa Cruz; sc40) for 45 min at room temperature and then with a secondary antibody (Invitrogen; A21428) for 1 h at room temperature. For F-actin immunofluorescent staining, cells were incubated with Phalloidin conjugated with Alexa Fluor 488 (1:500 dilution; Thermo Fisher Scientific; A12379) for 30 min at room

temperature as described before (Sinha *et al*, 2022). VECTASHIELD Antifade Mounting Medium with DAPI (Vector Laboratories; H-1200) was used to mount coverslips, and images were acquired with a Leica SP8 confocal microscope (Leica Microsystems).

Ubiquitination assay

HEK293T cells transfected with the indicated constructs and stable MDA-MB-231-HA-Ub cells were treated with 5 μ M MG132 for 5 h prior to harvesting. Cells were lysed in 1% SDS-RIPA buffer (25 mM Tris-HCl (pH 7.4), 150 mM NaCl, 1% NP40, 0.5% sodium deoxycholate, and 1% SDS) supplemented with a protease inhibitor and 10 mM N-ethylmaleimide (NEM; Sigma-Aldrich; E3876). After the lysates were boiled for 5 min and diluted to an SDS concentration of 0.1%, 20 μ l of anti-FLAG agarose (Sigma-Aldrich; A2220) was added to the lysates containing equal amounts of protein and incubated for 30 min at 4°C. To detect the polyubiquitination of endogenous T β RI, cell lysates were incubated with 5 μ l of an antibody against T β RI (Santa Cruz; sc-398) for 16 h at 4°C. The mixture was then incubated with 20 μ l of Protein A Sepharose (GE Healthcare; 17-0963-03) for 2 h at 4°C. After five washes, the beads were boiled in 2 \times sample buffer and analyzed by western blotting.

IncuCyte migration assays

For the wound healing migration assay, 5×10^4 MDA-MB-231 and A549 cells were seeded in the wells of an Essen ImageLock plate (Essen BioScience; 4379). After 16 h culture, the medium was replaced with DMEM supplemented with 0.5% FBS for another 8 h of culture. A WoundMaker tool (Essen BioScience) was used to generate scratch wounds, after which floating cells were washed away with PBS. An IncuCyte live cell imaging system (Essen BioScience) was used to monitor cell migration. For the chemotactic migration assay, 1×10^3 MDA-MB-231 or A549 cells in DMEM supplemented with 0.5% FBS were seeded in the upper chambers of an IncuCyte Clearview 96-well plate (Essen BioScience; 4582). Then, 200 μ l of DMEM supplemented with 10% FBS was added to the lower reservoir plate. Cells in the top and bottom chambers were imaged and quantified with the IncuCyte system.

Subcellular fractionation

Cells from a 10 cm dish were collected and lysed in 250 μ l of buffer A (50 mM Tris-HCl (pH 7.4), 150 mM NaCl, 1% NP40, and 0.25% sodium deoxycholate) for 15 min on ice. After centrifugation at 3,000 g for 5 min, the supernatant was collected and saved as the cytoplasmic fraction. The pellet was washed with PBS twice and resuspended in 150 μ l of buffer B (50 mM Tris-HCl (pH 7.4), 400 mM NaCl, 1% NP40, 0.5% sodium deoxycholate, and 1% SDS). After 20 min of incubation on ice and centrifugation at 12,000 g for 15 min, the supernatant was collected and saved as the nuclear fraction. The isolated cytoplasmic and nuclear fractions were used to quantify the expression of lncRNAs by RT-qPCR.

RACE

RACE was performed on A549 cells according to the manufacturer's instructions of a SMARTer RACE 5'/3' Kit (TaKaRa; 634859). In

brief, 5' and 3' RACE were carried out with specific primers on synthesized cDNA from A549 cells. After agarose gel electrophoresis, DNA was isolated and subcloned into the pRACE vector. Sanger sequencing was performed to analyze the sequence amplified from RACE.

RIP

To identify interactions between lncRNAs and proteins of interest, RIP was performed with a Magna RIP™ RNA-Binding Protein Immunoprecipitation Kit (Merck Millipore; 17-700). In brief, cells were collected and lysed in RIP lysis buffer. After centrifugation at 12,000 g for 10 min at 4°C, the supernatant was collected and supplemented with 700 µl of wash buffer and 50 µl of magnetic beads. After being precleared for 6 h at 4°C, the cell lysate was transferred to a new Eppendorf tube with 2.5 µg of an anti-FLAG antibody (Sigma–Aldrich; F1804), anti-SMURF2 antibody (Santa Cruz, sc-393848), anti-TβRI antibody (Santa Cruz, sc-398), or normal mouse/rabbit IgG and incubated for 16 h at 4°C. For *in vitro* RIP, 9 pmol of *in vitro*-transcribed *LITATS1-S* or *LITATS1-AS* was incubated with 1 pmol TβRI-ICD (CARNA BIOSCIENCES; 09-441-20N) for 16 h at 4°C. The beads were blocked with 5 µl of yeast tRNA (Invitrogen; AM7119) and 5 µl of BSA (Invitrogen; AM2618) for 2 h at 4°C and were then added to the cell lysates for another 3 h of incubation at 4°C. Then, the beads were treated with 1.5 µl of DNase I (Roche; 04716728001) for 10 min at 37°C followed by 1.5 µl of proteinase K (Merck Millipore; 71049) for 20 min at 56°C. RNA was extracted from the beads, and RT–qPCR was performed as mentioned above.

RNA pull-down assay

RNA pull-down assays were performed to identify *in vitro* interactions between lncRNAs and proteins of interest. In brief, a MEGA-script Kit (Thermo Fisher Scientific; AM1334) was used to synthesize antisense and sense *LITATS1* through *in vitro* transcription. Next, RNA was extracted, and 50 pmol of antisense or sense *LITATS1* was biotinylated with an RNA 3' End Desthiobiotinylation Kit (Thermo Fisher Scientific; 20160). The tertiary structure of each lncRNA was recovered by 10 min of incubation at 70°C followed by gradual cooling to room temperature. HEK293T cell lysates and recombinant FLAG-SMURF1 protein (Sigma–Aldrich; SRP0227) or recombinant FLAG-SMURF2 protein (Sigma–Aldrich; SRP0228) were incubated with biotinylated lncRNA for 16 h at 4°C. Magnetic beads from a Magnetic RNA–Protein Pull-Down Kit (Thermo Fisher Scientific; 20164) were utilized to capture RNA–protein complexes. Proteins were eluted from the beads and analyzed by western blotting.

CARPID

The CARPID approach was utilized to validate interactions between lncRNAs and proteins of interest at the endogenous level. In brief, biotin (Sigma–Aldrich; B4639) was added to the medium at a final concentration of 200 µM to activate biotinylation for 30 min at 37°C. Cells were collected and lysed in TNE lysis buffer (50 mM Tris–HCl (pH 7.4), 1 mM EDTA, 150 mM NaCl, and 1% NP40) on ice for 10 min. Then, 20 µl of NeutrAvidin™ Agarose (Thermo Fisher Scientific; 29200) was added to the cell lysates with the same

amount of protein. The beads were washed with TNE buffer 5 times after incubation for 16 h at 4°C and were then boiled for 5 min in 2× sample buffer. Western blotting was carried out to analyze the enrichment of biotinylated proteins.

PLA

To analyze the endogenous interactions between *LITATS1* and TβRI or SMURF2, a PLA was performed. In brief, A549 cells were seeded on coverslips in the wells of a 24-well plate. After serum starvation for 16 h, the cells were stimulated with or without TGF-β (5 ng/ml) for 2 h. Subsequently, the cells were fixed with 4% PFA for 10 min and permeabilized with PBS supplemented with 0.5% Triton-X for 5 min. The cells were then blocked with Duolink® Blocking Solution for 1 h at 37°C and incubated with primary antibodies against TβRI (Santa Cruz; sc-398) and SMURF2 (Santa Cruz; sc-393848) at a 1:500 dilution for 16 h at 4°C. After three washes with wash buffer A (Sigma–Aldrich; DUO82049), the cells were incubated with secondary antibodies conjugated to the PLUS and MINUS PLA probes (Sigma–Aldrich; DUO92001 and DUO92005) for 1 h at 37°C. Then, ligase (Sigma–Aldrich; DUO92008) was added to the cells and incubated for 30 min prior to incubation with Duolink® Polymerase (Sigma–Aldrich; Cat. Nr.: DUO82028) for 90 min at 37°C. After three washes with wash buffer B (Sigma–Aldrich; Cat. Nr.: DUO82048), the samples were mounted with VECTASHIELD Antifade Mounting Medium with DAPI (Vector Laboratories; H-1200), and images were acquired with a Leica SP8 confocal microscope (Leica Microsystems).

Flow cytometry

Vimentin expression in A549-VIM-RFP cells was quantified by RFP-directed flow cytometry as described elsewhere (Wang *et al*, 2021). In brief, A549-VIM-RFP stable cells were collected, washed with PBS, and resuspended in PBS containing 5% BSA and 2 mM EDTA (pH 8.0). Subsequently, at least 10,000 cells were acquired with a BD LSR II flow cytometer (BD Biosciences), and the results were analyzed with FlowJo 10.5.0 software.

RNA-seq-based transcriptional profiling, pathway enrichment analysis, and GSEA

To screen for lncRNAs induced by TGF-β, MCF10A-M1, MCF10A-M2, and MDA-MB-231 cells (in biological triplicate) were serum starved for 16 h and stimulated with TGF-β (5 ng/ml) for 0, 2, 8, and 24 h. Then, total RNA was isolated from the cells with TRIzol reagent (Thermo Fisher Scientific; 15596026). Libraries were constructed, and transcriptional analysis was performed on the Illumina HiSeq platform (Beijing Genomics Institute (BGI), Shenzhen). Bioinformatic analysis of differentially expressed transcripts was carried out by BGI. To screen for mRNAs affected by *LITATS1*, we transduced A549 cells with constructs expressing two independent shRNAs (sh*LITATS1* #1 and sh*LITATS1* #2) or a nontargeting shRNA (Co.sh). After oligo(dT) selection and library preparation, the DNBSeq platform (BGI, Hong Kong) was used to perform RNA-seq. RNA-seq files were processed using the open-source BIODWDL RNAseq pipeline v4.0.0 (<https://zenodo.org/record/3975552#>. YiBgxIzMKV4) developed at Leiden University Medical Center

(LUMC). This pipeline performs FASTQ preprocessing (including quality control, quality trimming, and adapter clipping), RNA-seq alignment, read quantification, and optional transcript assembly. FastQC was used for QC checks on raw reads. Adapter clipping was performed using Cutadapt (v2.10) with default settings. RNA-seq read alignment was performed using STAR (v2.7.5a) with the GRCh38 human reference genome. Gene reads were quantified using HTSeq-count (v0.12.4) with the “–stranded = no” setting. The Ensembl version 99 gene annotation was used for quantification. Differential gene expression analysis was performed using R (v3.6.3). First, the gene read count matrix was used to calculate the counts per million mapped reads (CPM) per sample for all annotated genes. Genes with a log₂CPM higher than 1 in at least 25% of all samples were retained for downstream analysis. The numbers of retained genes for each comparison were as follows: Co.sh vs. shLITATS1 #1, 12,646 genes; Co.sh vs. shLITATS1 #2, 12,692 genes; Co.sh –TGF-β vs. Co.sh +TGF-β, 12,858 genes. For differential gene expression analysis, the dgeAnalysis R-Shiny application (<https://github.com/LUMC/dgeAnalysis/tree/v1.3.1>) was used. EdgeR (v3.28.1) with trimmed mean of M values (TMM) normalization was used to perform differential gene expression analysis. The Benjamini–Hochberg false discovery rate (FDR) was computed to adjust the P-values obtained for each differentially expressed gene. Using a cutoff of 0.05 for the adjusted P-values, up- and downregulated genes were identified. The details of up- and downregulated lncRNAs in response to TGF-β stimulation and the differentially expressed genes upon LITATS1 depletion were shown in Appendix Tables S1 and S6, respectively. In order to investigate which splice variants of ZC3H12A-DT were expressed out of seven splice variants annotated in Ensembl gene annotation version 108, we estimated the raw sequencing reads using StringTie (v1.3.6) that can discriminate the seven splice variants. GSEA was performed with GSEA software (Subramanian et al, 2005). The TGF-β (TGFB_UP.V1_UP) gene response signature (Padua et al, 2008) and EMT (GOBP_EPITHELIAL_TO_MESENCHYMAL_TRANSITION; GO: 0001837) gene signature were used to evaluate the correlations between LITATS1 and TGF-β/SMAD signaling and EMT, respectively.

Differential gene expression and survival analyses based on patient samples

Differential expression of LITATS1 was analyzed in samples from patients with breast cancer of different subtypes from TCGA and GTEx datasets using the GEPIA2 database (Tang et al, 2019). Patient survival analysis was performed on the Kaplan–Meier Plotter website (<https://kmplot.com/analysis/>; Lanczky & Gyorffy, 2021). More details about the databases can be found in Appendix Table S7.

In situ hybridization staining

An RNAScope® Multiplex Fluorescent Kit (Advanced Cell Diagnostics; 323100) and an *in situ* probe for LITATS1 (Advanced Cell Diagnostics; 835371-C2) were utilized to evaluate the expression and localization of LITATS1 in A549 and MDA-MB-231 cells. All fluorescence *in situ* hybridization procedures were carried out strictly according to the manufacturer's instructions. Images were acquired with a DMi8 inverted fluorescence microscope (Leica). To analyze LITATS1 expression in patient samples, *in situ* hybridization was performed on tissue

microarrays using a 2.5 HD Detection Kit—BROWN (Advanced Cell Diagnostics; 322300) and the same *in situ* probe mentioned above. A tissue microarray with lung adenocarcinoma and matched lung tissues was purchased from Biomax (LC1504), and a breast cancer tissue microarray was constructed from the ORIGO cohort (Leiden University Medical Center), which includes 175 breast cancer patients. Patients included in this cohort were diagnosed with a primary breast tumor and treated in the Leiden University Medical Center (LUMC) between 1997 and 2003 (Out et al, 2012). Informed consent was obtained from all patients. All *in situ* hybridization procedures were carried out strictly following the manufacturer's instructions for the 2.5 HD Detection Kit—BROWN. Images were acquired with a digital slide scanner (Pannoramic 250 Flash III, 3DHISTECH). The staining index was quantified by the following formula: staining intensity (0, no staining; 1, light brown; 2, brown; 3, dark brown) × proportion of positive cells (0, no positive cells; 1, < 10%; 2, 10–50%; 3, > 50%). The scores were given in a blind manner.

Embryonic zebrafish extravasation assay

The experiments were conducted in a licensed establishment for the breeding and use of experimental animals (LU) and subject to internal regulations and guidelines, stating that advice is taken from the animal welfare body to minimize suffering for all experimental animals housed at the facility. The zebrafish assays described are not considered an animal experiment under the Experiments on Animals Act (Wod, effective 2014), the applicable legislation in the Netherlands in accordance with the European guidelines (EU directive no. 2010/63/EU) regarding the protection of animals used for scientific purposes, because non-self-eating larvae were used. Therefore a license specific for these assays on zebrafish larvae (< 5d) was not required. MDA-MB-231 cells labeled with mCherry were injected into the duct of Cuvier of embryos from transgenic zebrafish (*flt1*; EGFP) as previously described (Ren et al, 2017). After being maintained in 33°C egg water for 5 days, zebrafish embryos were fixed with 4% formaldehyde. An inverted SP5 STED confocal microscope (Leica) was used to visualize the injected cancer cells and zebrafish embryos. At least 30 embryos per group were analyzed. Two independent experiments were performed, and representative results are shown.

Statistical analysis

Statistical analysis was performed using GraphPad Prism 9. The unpaired Student's *t*-test was used for most analyses, and *P* < 0.05 was considered statistically significant. All measurements in this study were taken from distinct samples.

Data availability

The RNA-seq data from this publication have been deposited to the GEO database and assigned the identifier GSE203119 (<https://www.ncbi.nlm.nih.gov/geo/query/acc.cgi?acc=GSE203119>) and GSE198393 (<https://www.ncbi.nlm.nih.gov/geo/query/acc.cgi?acc=GSE198393>).

Expanded View for this article is available [online](#).

Acknowledgements

We acknowledge the support of the Chinese Scholarship Council (CSC) to Chuannan Fan and Qian Wang and the Cancer Genomics Centre in the Netherlands (CGC. NL) and the ZonMW grant (09120012010061) to Peter ten Dijke. We thank Midory Thorikay, Maarten van Dinther, and Martijn Rabelink for excellent technical assistance and Slobodan Vukicevic (University of Zagreb, Croatia) and Andrew Hinck (University of Pittsburgh, USA) for generously providing human recombinant BMP6 and TGF- β 3, respectively. We acknowledge all other members of the ten Dijke laboratory and Yuva Oz for their kind support.

Author contributions

Chuannan Fan: Conceptualization; investigation; methodology; writing – original draft; writing – review and editing. **Qian Wang:** Investigation. **Thomas B Kuipers:** Investigation. **Davy Cats:** Investigation; methodology. **Prasanna Vasudevan Iyengar:** Conceptualization. **Sophie C Hagenaars:** Investigation. **Wilma E Mesker:** Investigation. **Peter Devilee:** Investigation. **Rob A E M Tollenaar:** Investigation. **Hailiang Mei:** Investigation; methodology. **Peter ten Dijke:** Conceptualization; supervision; writing – original draft; project administration; writing – review and editing.

Disclosure and competing interests statement

The authors declare that they have no conflict of interest.

References

- Beylerli O, Gareev I, Sufianov A, Ilyasova T, Guang Y (2022) Long noncoding RNAs as promising biomarkers in cancer. *Noncoding RNA Res* 7: 66–70
- Budi EH, Duan D, Derynck R (2017) Transforming growth factor- β receptors and Smads: regulatory complexity and functional versatility. *Trends Cell Biol* 27: 658–672
- Cantiello F, Russo GI, Cicione A, Ferro M, Cimino S, Favilla V, Perdona S, De Cobelli O, Magno C, Morgia G et al (2016) PHI and PCA3 improve the prognostic performance of PRIAS and Epstein criteria in predicting insignificant prostate cancer in men eligible for active surveillance. *World J Urol* 34: 485–493
- Cheng D, Xu Q, Liu Y, Li G, Sun W, Ma D, Ni C (2021) Long noncoding RNA-SNHG20 promotes silica-induced pulmonary fibrosis by miR-490-3p/TGFBR1 axis. *Toxicology* 451: 152683
- Chung VY, Tan TZ, Ye JR, Huang RL, Lai HC, Kappei D, Wollmann H, Guccione E, Huang RYJ (2019) The role of GRHL2 and epigenetic remodeling in epithelial-mesenchymal plasticity in ovarian cancer cells. *Commun Biol* 2: 272
- Colak S, ten Dijke P (2017) Targeting TGF- β signaling in cancer. *Trends Cancer* 3: 56–71
- Dennler S, Itoh S, Vivien D, ten Dijke P, Huet S, Gauthier JM (1998) Direct binding of Smad3 and Smad4 to critical TGF β -inducible elements in the promoter of human plasminogen activator inhibitor-type 1 gene. *EMBO J* 17: 3091–3100
- Dongre A, Weinberg RA (2019) New insights into the mechanisms of epithelial-mesenchymal transition and implications for cancer. *Nat Rev Mol Cell Biol* 20: 69–84
- Du Y, Yang H, Li Y, Guo W, Zhang Y, Shen H, Xing L, Li Y, Wu W, Zhang X (2021) Long non-coding RNA LINC01137 contributes to oral squamous cell carcinoma development and is negatively regulated by miR-22-3p. *Cell Oncol (Dordr)* 44: 595–609
- Fan C, Zhang J, Hua W, ten Dijke P (2018) Biphasic role of TGF- β in cancer progression: from tumor suppressor to tumor promotor. In *Encyclopedia of cancer*, 3rd edn. Amsterdam: Elsevier Press
- Fan C, Wang Q, van der Zon G, Ren J, Agaser C, Sliker RC, Iyengar PV, Mei H, ten Dijke P (2022) OVOL1 inhibits breast cancer cell invasion by enhancing the degradation of TGF- β type I receptor. *Signal Transduct Target Ther* 7: 126
- Ferro M, Lucarelli G, Bruzzese D, Perdona S, Mazzarella C, Perruolo G, Marino A, Cosimato V, Giorgio E, Tagliamonte V et al (2015) Improving the prediction of pathologic outcomes in patients undergoing radical prostatectomy: the value of prostate cancer antigen 3 (PCA3), prostate health index (phi) and sarcosine. *Anticancer Res* 35: 1017–1023
- Groskopf J, Aubin SMJ, Deras IL, Blase A, Bodrug S, Clark C, Brentano S, Mathis J, Pham J, Meyer T et al (2006) APTIMA PCA3 molecular urine test: development of a method to aid in the diagnosis of prostate cancer. *Clin Chem* 52: 1089–1095
- Gui P, Bivona TG (2022) Evolution of metastasis: new tools and insights. *Trends Cancer* 8: 98–109
- Gyorffy B (2021) Survival analysis across the entire transcriptome identifies biomarkers with the highest prognostic power in breast cancer. *Comput Struct Biotechnol J* 19: 4101–4109
- Gyorffy B, Surowiak P, Budczies J, Lanczky A (2014) Online survival analysis software to assess the prognostic value of biomarkers using transcriptomic data in non-small-cell lung cancer. *PLoS One* 8: e82241
- Hanahan D (2022) Hallmarks of cancer: new dimensions. *Cancer Discov* 12: 31–46
- Hao Y, Baker D, ten Dijke P (2019) TGF- β -mediated epithelial-mesenchymal transition and cancer metastasis. *Int J Mol Sci* 20: 2767
- Hata A, Chen YG (2016) TGF- β signaling from receptors to Smads. *Cold Spring Harb Perspect Biol* 8: a022061
- Hu W, Qin L, Li M, Pu X, Guo Y (2018) A structural dissection of protein-RNA interactions based on different RNA base areas of interfaces. *RSC Adv* 8: 10582–10592
- Hu H, Fu Y, Zhou B, Li Z, Liu Z, Jia Q (2021) Long non-coding RNA TCONS_00814106 regulates porcine granulosa cell proliferation and apoptosis by sponging miR-1343. *Mol Cell Endocrinol* 520: 111064
- Ickenstein LM, Garidel P (2019) Lipid-based nanoparticle formulations for small molecules and RNA drugs. *Expert Opin Drug Deliv* 16: 1205–1226
- Jarroux J, Foretek D, Bertrand C, Gabriel M, Szachnowski U, Saci Z, Guo S, Londono-Vallejo A, Pinskaya M, Morillon A (2021) HOTAIR lncRNA promotes epithelial-mesenchymal transition by redistributing LSD1 at regulatory chromatin regions. *EMBO Rep* 22: e50193
- Jin J, Jia ZH, Luo XH, Zhai HF (2020) Long non-coding RNA HOXA11-AS accelerates the progression of keloid formation via miR-124-3p/TGFBR1 axis. *Cell Cycle* 19: 218–232
- Kang Y, Chen CR, Massague J (2003) A self-enabling TGF β response coupled to stress signaling: Smad engages stress response factor ATF3 for Id1 repression in epithelial cells. *Mol Cell* 11: 915–926
- Katsuno Y, Lamouille S, Derynck R (2013) TGF- β signaling and epithelial-mesenchymal transition in cancer progression. *Curr Opin Oncol* 25: 76–84
- Kavak P, Rasmussen RK, Causing CG, Bonni S, Zhu H, Thomsen GH, Wrana JL (2000) Smad7 binds to Smurf2 to form an E3 ubiquitin ligase that targets the TGF β receptor for degradation. *Mol Cell* 6: 1365–1375
- Kishore S, Jaskiewicz L, Burger L, Hausser J, Khorshid M, Zavolan M (2011) A quantitative analysis of CLIP methods for identifying binding sites of RNA-binding proteins. *Nat Methods* 8: 559–564
- Koboldt DC, Fulton RS, McLellan MD, Schmidt H, Kalicki-Weizer J, McMichael JF, Fulton LL, Dooling DJ, Ding L, Mardis ER et al (2012) Comprehensive molecular portraits of human breast tumours. *Nature* 490: 61–70

- Lanczky A, Györfy B (2021) Web-based survival analysis tool tailored for medical research (KMplot): development and implementation. *J Med Internet Res* 23: e27633
- Laping NJ, Grygielko E, Mathur A, Butter S, Bomberger J, Tweed C, Martin W, Fornwald J, Lehr R, Harling J et al (2002) Inhibition of transforming growth factor (TGF)- β 1-induced extracellular matrix with a novel inhibitor of the TGF- β type I receptor kinase activity: SB-431542. *Mol Pharmacol* 62: 58–64
- Li Y, Liu G, Li X, Dong H, Xiao W, Lu S (2018) Long non-coding RNA SBF2-AS1 promotes hepatocellular carcinoma progression through regulation of miR-140-5p-TGFBR1 pathway. *Biochem Biophys Res Commun* 503: 2826–2832
- Li Y, Zhao Z, Sun D, Li Y (2021) Novel long noncoding RNA LINC02323 promotes cell growth and migration of ovarian cancer via TGF- β receptor 1 by miR-1343-3p. *J Clin Lab Anal* 35: e23651
- Lin C, Yang L (2018) Long noncoding RNA in cancer: wiring signaling circuitry. *Trends Cell Biol* 28: 287–301
- Liu B, Sun L, Liu Q, Gong C, Yao Y, Lv X, Lin L, Yao H, Su F, Li D et al (2015) A cytoplasmic NF- κ B interacting long noncoding RNA blocks I κ B phosphorylation and suppresses breast cancer metastasis. *Cancer Cell* 27: 370–381
- Liu S, Gonzalez-Prieto R, Zhang M, Geurink PP, Kooij R, Iyengar PV, van Dinther M, Bos E, Zhang X, Le Devedec SE et al (2020) Deubiquitinase activity profiling identifies UCHL1 as a candidate oncoprotein that promotes TGF β -induced breast cancer metastasis. *Clin Cancer Res* 26: 1460–1473
- Lonsdale J, Thomas J, Salvatore M, Phillips R, Lo E, Shad S, Hasz R, Walters G, Garcia F, Young N et al (2013) The genotype-tissue expression (GTEx) project. *Nat Genet* 45: 580–585
- Lourenco AR, Roukens MG, Seinstra D, Frederiks CL, Pals CE, Vervoort SJ, Margarido AS, van Rheenen J, Coffey PJ (2020) C/EBP α is crucial determinant of epithelial maintenance by preventing epithelial-to-mesenchymal transition. *Nat Commun* 11: 785
- Lu Z, Li Y, Wang J, Che Y, Sun S, Huang J, Chen Z, He J (2017) Long non-coding RNA NKILA inhibits migration and invasion of non-small cell lung cancer via NF- κ B/Snail pathway. *J Exp Clin Cancer Res* 36: 54
- Lutz J, Lazzaro S, Habbeddine M, Schmidt KE, Baumhof P, Mui BL, Tam YK, Madden TD, Hope MJ, Heidenreich R et al (2017) Unmodified mRNA in LNPs constitutes a competitive technology for prophylactic vaccines. *NPJ Vaccines* 2: 29
- Ma Q, Yang L, Tolentino K, Wang G, Zhao Y, Litzenburger UM, Shi Q, Zhu L, Yang C, Jiao H et al (2022) Inducible lncRNA transgenic mice reveal continual role of HOTAIR in promoting breast cancer metastasis. *Elife* 11: e79126
- Massague J, Gomis RR (2006) The logic of TGF β signaling. *FEBS Lett* 580: 2811–2820
- Mattick JS, Rinn JL (2015) Discovery and annotation of long noncoding RNAs. *Nat Struct Mol Biol* 22: 5–7
- Nakao A, Afrakhte M, Moren A, Nakayama T, Christian JL, Heuchel R, Itoh S, Kawabata M, Heldin NE, Heldin CH et al (1997) Identification of Smad7, a TGF β -inducible antagonist of TGF- β signalling. *Nature* 389: 631–635
- Nandwani A, Rathore S, Datta M (2021) lncRNAs in cancer: regulatory and therapeutic implications. *Cancer Lett* 501: 162–171
- Out AA, Wasielewski M, Huijts PEA, van Minderhout IJHM, Houwing-Duistermaat JJ, Tops CMJ, Nielsen M, Seynaeve C, Wijnen JT, Breuning MH et al (2012) MUTYH gene variants and breast cancer in a Dutch case-control study. *Breast Cancer Res Treat* 134: 219–227
- Padua D, Zhang XHF, Wang Q, Nadal C, Gerald WL, Gomis RR, Massague J (2008) TGF β primes breast tumors for lung metastasis seeding through angiopoietin-like 4. *Cell* 133: 66–77
- Palazzo AF, Koonin EV (2020) Functional long non-coding RNAs evolve from junk transcripts. *Cell* 183: 1151–1161
- Papoutsoglou P, Moustakas A (2020) Long non-coding RNAs and TGF- β signaling in cancer. *Cancer Sci* 111: 2672–2681
- Papoutsoglou P, Tsubakihara Y, Caja L, Moren A, Pallis P, Ameer A, Heldin CH, Moustakas A (2019) The TGF β 2-AS1 lncRNA regulates TGF- β signaling by modulating corepressor activity. *Cell Rep* 28: 3182–3198
- Parker JS, Mullins M, Cheang MCU, Leung S, Voduc D, Vickery T, Davies S, Fauron C, He X, Hu Z et al (2009) Supervised risk predictor of breast cancer based on intrinsic subtypes. *J Clin Oncol* 27: 1160–1167
- Pastushenko I, Blanpain C (2019) EMT transition states during tumor progression and metastasis. *Trends Cell Biol* 29: 212–226
- Qi J, Wu Y, Zhang H, Liu Y (2021) lncRNA NORAD regulates scar hypertrophy via miRNA-26a mediating the regulation of TGF β R1/2. *Adv Clin Exp Med* 30: 395–403
- Ren J, Liu S, Cui C, ten Dijke P (2017) Invasive behavior of human breast cancer cells in embryonic zebrafish. *J Vis Exp* 122: 55459
- Richards EJ, Zhang G, Li ZP, Permut-Wey J, Challa S, Li Y, Kong W, Dan S, Bui MM, Coppola D et al (2015) Long non-coding RNAs (lncRNA) regulated by transforming growth factor (TGF) β : lncRNA-hit-mediated TGF β -induced epithelial to mesenchymal transition in mammary epithelia. *J Biol Chem* 290: 6857–6867
- Sakai S, Ohhata T, Kitagawa K, Uchida C, Aoshima T, Niida H, Suzuki T, Inoue Y, Miyazawa K, Kitagawa M (2019) Long noncoding RNA ELIT-1 acts as a Smad3 cofactor to facilitate TGF β /Smad signaling and promote epithelial-mesenchymal transition. *Cancer Res* 79: 2821–2838
- Sanchez de Groot N, Armaos A, Grana-Montes R, Alriquet M, Calloni G, Vabulas RM, Tartaglia GG (2019) RNA structure drives interaction with proteins. *Nat Commun* 10: 3246
- Sha Y, Haensel D, Gutierrez G, Du H, Dai X, Nie Q (2019) Intermediate cell states in epithelial-to-mesenchymal transition. *Phys Biol* 16: 021001
- Shibue T, Weinberg RA (2017) EMT, CSCs, and drug resistance: the mechanistic link and clinical implications. *Nat Rev Clin Oncol* 14: 611–629
- Sinha A, Mehta P, Fan C, Zhang J, Marvin DL, van Dinther M, Ritsma L, Boukany PE, ten Dijke P (2022) Visualizing dynamic changes during TGF- β -induced epithelial to mesenchymal transition. *Methods Mol Biol* 2488: 47–65
- van Staalduinen J, Baker D, ten Dijke P, van Dam H (2018) Epithelial-mesenchymal-transition-inducing transcription factors: new targets for tackling chemoresistance in cancer? *Oncogene* 37: 6195–6211
- Statello L, Guo CJ, Chen LL, Huarte M (2021) Gene regulation by long non-coding RNAs and its biological functions. *Nat Rev Mol Cell Biol* 22: 96–118
- Subramanian A, Tamayo P, Mootha VK, Mukherjee S, Ebert BL, Gillette MA, Paulovich A, Pomeroy SL, Golub TR, Lander ES et al (2005) Gene set enrichment analysis: a knowledge-based approach for interpreting genome-wide expression profiles. *Proc Natl Acad Sci U S A* 102: 15545–15550
- Tang Z, Kang B, Li C, Chen T, Zhang Z (2019) GEPIA2: an enhanced web server for large-scale expression profiling and interactive analysis. *Nucleic Acids Res* 47: W556–W560
- Tani H, Numajiri A, Aoki M, Umemura T, Nakazato T (2019) Short-lived long noncoding RNAs as surrogate indicators for chemical stress in HepG2 cells and their degradation by nuclear RNases. *Sci Rep* 9: 20299
- Tay Y, Rinn J, Pandolfi PP (2014) The multilayered complexity of ceRNA crosstalk and competition. *Nature* 505: 344–352

- Thomson DW, Dinger ME (2016) Endogenous microRNA sponges: evidence and controversy. *Nat Rev Genet* 17: 272–283
- Tian H, Lian R, Li Y, Liu C, Liang S, Li W, Tao T, Wu X, Ye Y, Yang X et al (2020) AKT-induced lncRNA VAL promotes EMT-independent metastasis through diminishing Trim16-dependent vimentin degradation. *Nat Commun* 11: 5127
- Tzavlaki K, Moustakas A (2020) TGF- β signaling. *Biomolecules* 10: 487
- Wang L, Park HJ, Dasari S, Wang S, Kocher JP, Li W (2013) CPAT: coding-potential assessment tool using an alignment-free logistic regression model. *Nucleic Acids Res* 41: e74
- Wang P, Luo ML, Song E, Zhou Z, Ma T, Wang J, Jia N, Wang G, Nie S, Liu Y et al (2018) Long noncoding RNA lnc-TSI inhibits renal fibrogenesis by negatively regulating the TGF- β /Smad3 pathway. *Sci Transl Med* 10: eaat2039
- Wang Q, Liu J, Janssen JM, Le Bouteiller M, Frock RL, Goncalves MAFV (2021) Precise and broad scope genome editing based on high-specificity Cas9 nickases. *Nucleic Acids Res* 49: 1173–1198
- Watanabe K, Villarreal-Ponce A, Sun P, Salmans ML, Fallahi M, Andersen B, Dai X (2014) Mammary morphogenesis and regeneration require the inhibition of EMT at terminal end buds by *Ovol2* transcriptional repressor. *Dev Cell* 29: 59–74
- Wu W, Chen F, Cui X, Yang L, Chen J, Zhao J, Huang D, Liu J, Yang L, Zeng J et al (2018) lncRNA NKILA suppresses TGF- β -induced epithelial-mesenchymal transition by blocking NF- κ B signaling in breast cancer. *Int J Cancer* 143: 2213–2224
- Xu L, Liu W, Li T, Hu Y, Wang Y, Huang L, Wang Y, Shao S, Liu X, Zhan Q (2021) Long non-coding RNA SMASR inhibits the EMT by negatively regulating TGF- β /Smad signaling pathway in lung cancer. *Oncogene* 40: 3578–3592
- Yan X, Xiong X, Chen YG (2018) Feedback regulation of TGF- β signaling. *Acta Biochim Biophys Sin (Shanghai)* 50: 37–50
- Yang G, Lin C (2020) Long noncoding RNA SOX2-OT exacerbates hypoxia-induced cardiomyocytes injury by regulating miR-27a-3p/TGF β 1 Axis. *Cardiovasc Ther* 2020: 2016259
- Yang J, Antin P, Bex G, Blanpain C, Brabletz T, Bronner M, Campbell K, Cano A, Casanova J, Christofori G et al (2020) Guidelines and definitions for research on epithelial-mesenchymal transition. *Nat Rev Mol Cell Biol* 21: 341–352
- Yi W, Li J, Zhu X, Wang X, Fan L, Sun W, Liao L, Zhang J, Li X, Ye J et al (2020) CRISPR-assisted detection of RNA-protein interactions in living cells. *Nat Methods* 17: 685–688
- Yoon JH, Abdelmohsen K, Kim J, Yang X, Martindale JL, Tominaga-Yamanaka K, White EJ, Orjalo AV, Rinn JL, Kreft SG et al (2013) Scaffold function of long non-coding RNA HOTAIR in protein ubiquitination. *Nat Commun* 4: 2939
- Yuan JH, Yang F, Wang F, Ma JZ, Guo YJ, Tao QF, Liu F, Pan W, Wang TT, Zhou CC et al (2014) A long noncoding RNA activated by TGF- β promotes the invasion-metastasis cascade in hepatocellular carcinoma. *Cancer Cell* 25: 666–681
- Zhou B, Guo W, Sun C, Zhang B, Zheng F (2018) linc00462 promotes pancreatic cancer invasiveness through the miR-665/TGFBR1-TGFBR2/SMAD2/3 pathway. *Cell Death Dis* 9: 706
- Zhu L, Liu Y, Tang H, Wang P (2022) FOXP3 activated-LINC01232 accelerates the stemness of non-small cell lung carcinoma by activating TGF- β signaling pathway and recruiting IGF2BP2 to stabilize TGFBR1. *Exp Cell Res* 413: 113024



License: This is an open access article under the terms of the [Creative Commons Attribution-NonCommercial-NoDerivs](https://creativecommons.org/licenses/by-nc-nd/4.0/) License, which permits use and distribution in any medium, provided the original work is properly cited, the use is non-commercial and no modifications or adaptations are made.